

Climate change projections for Tasman and impacts on agricultural systems

Prepared for Tasman District Council/Envirolink

October 2019

Prepared by:
Petra Pearce
John-Mark Woolley
Abha Sood

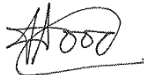
For any information regarding this report please contact:

Petra Pearce
Manager - Climate, Atmosphere and Hazards
Climate and Environmental Applications
+64-9-375 2052
petra.pearce@niwa.co.nz

National Institute of Water & Atmospheric Research Ltd
Private Bag 99940
Viaduct Harbour
Auckland 1010

Phone +64 9 375 2050

NIWA CLIENT REPORT No: 2019309AK
Report date: October 2019
NIWA Project: ELF20101/ELF20102

Quality Assurance Statement		
	Reviewed by:	Dr Abha Sood Climate Scientist NIWA - Wellington
	Formatting checked by:	Petra Pearce
	Approved for release by:	Jonathan Moores Regional Manager NIWA – Auckland

© All rights reserved. This publication may not be reproduced or copied in any form without the permission of the copyright owner(s). Such permission is only to be given in accordance with the terms of the client's contract with NIWA. This copyright extends to all forms of copying and any storage of material in any kind of information retrieval system.

Whilst NIWA has used all reasonable endeavours to ensure that the information contained in this document is accurate, NIWA does not give any express or implied warranty as to the completeness of the information contained herein, or that it will be suitable for any purpose(s) other than those specifically contemplated during the Project or agreed by NIWA and the Client.

Contents

- Executive summary 6**
- 1 Introduction 7**
- 2 Methodology 7**
- 3 Heatwave day projections 8**
- 4 Growing degree day projections 12**
- 5 Heavy rain day projections (> 25 mm) 16**
- 6 Extreme rainfall projections (HIRDS v4) 27**
- 7 Potential evapotranspiration deficit projections (meteorological drought) 35**
- 8 Soil moisture deficit day projections 38**
- 9 Climate change impacts on agricultural systems 49**
 - 9.1 Heat impacts 51
 - 9.2 Drought impacts 52
 - 9.3 Heavy rainfall impacts 52
- 10 Summary 53**
- 11 References 54**
- Appendix A Climate modelling methodology 55**
- Appendix B Representative Concentration Pathways 57**

Tables

- Table 6-1: Extreme rainfall projections for Bainham, from HIRDS v4. 29
- Table 6-2: Extreme rainfall projections for Takaka, from HIRDS v4. 30
- Table 6-3: Extreme rainfall projections for Motueka (Riwaka), from HIRDS v4. 31
- Table 6-4: Extreme rainfall projections for Appleby, from HIRDS v4. 32
- Table 6-5: Extreme rainfall projections for Motupiko, from HIRDS v4. 33
- Table 6-6: Extreme rainfall projections for Lake Rotoiti, from HIRDS v4. 34
- Table 9-1: Tasman District's productive land classes. 49
- Table 11-1: Projected change in global mean surface air temperature for the mid- and late-21st century relative to the reference period of 1986-2005 for different RCPs. 58

Figures

Figure 3-1:	Modelled annual number of heatwave days (\geq three consecutive days with maximum temperatures $> 25^{\circ}\text{C}$), average over the historic period 1986-2005.	9
Figure 3-2:	Projected annual heatwave day changes (number of days within periods of \geq three consecutive days with maximum temperatures $> 25^{\circ}\text{C}$) at 2040 and 2090.	10
Figure 3-3:	Projected annual total number of heatwave days (number of days within periods of \geq three consecutive days with maximum temperatures $> 25^{\circ}\text{C}$) at 2040 and 2090.	11
Figure 4-1:	Modelled annual number of growing degree days (base 10°C), average over the historic period 1986-2005.	13
Figure 4-2:	Projected annual growing degree day changes (base 10°C) at 2040 and 2090.	14
Figure 4-3:	Projected total number of annual growing degree days (base 10°C) at 2040 and 2090.	15
Figure 5-1:	Modelled annual number of heavy rain days ($>25\text{mm}$) (average over the historic period 1986-2005).	17
Figure 5-2:	Modelled seasonal number of heavy rain days ($>25\text{mm}$) (average over the historic period 1986-2005).	18
Figure 5-3:	Projected change in annual number of heavy rain days ($>25\text{mm}$) by 2040 for RCP4.5.	19
Figure 5-4:	Projected change in seasonal number of heavy rain days ($>25\text{mm}$) by 2040 for RCP4.5.	20
Figure 5-5:	Projected change in annual number of heavy rain days ($>25\text{mm}$) by 2040 for RCP8.5.	21
Figure 5-6:	Projected change in seasonal number of heavy rain days ($>25\text{mm}$) by 2040 for RCP8.5.	22
Figure 5-7:	Projected change in annual number of heavy rain days ($>25\text{mm}$) by 2090 for RCP4.5.	23
Figure 5-8:	Projected change in seasonal number of heavy rain days ($>25\text{mm}$) by 2090 for RCP4.5.	24
Figure 5-9:	Projected change in annual number of heavy rain days ($>25\text{mm}$) by 2090 for RCP8.5.	25
Figure 5-10:	Projected change in seasonal number of heavy rain days ($>25\text{mm}$) by 2090 for RCP8.5.	26
Figure 6-1:	Locations/station network numbers for HIRDS rainfall analysis.	28
Figure 7-1:	Modelled annual accumulated Potential Evapotranspiration Deficit (mm), average over 1986-2005.	36
Figure 7-2:	Projected annual change in accumulated Potential Evapotranspiration Deficit (mm) at 2040 and 2090.	37
Figure 8-1:	Modelled annual number of days of soil moisture deficit (average over the historic period 1986-2005).	39
Figure 8-2:	Modelled seasonal number of days of soil moisture deficit (average over the historic period 1986-2005).	40
Figure 8-3:	Projected change in annual number of days of soil moisture deficit by 2040 for RCP4.5.	41
Figure 8-4:	Projected change in seasonal number of days of soil moisture deficit by 2040 for RCP4.5.	42

Figure 8-5: Projected change in annual number of days of soil moisture deficit by 2040 for RCP8.5.	43
Figure 8-6: Projected change in seasonal number of days of soil moisture deficit by 2040 for RCP8.5.	44
Figure 8-7: Projected change in annual number of days of soil moisture deficit by 2090 for RCP4.5.	45
Figure 8-8: Projected change in seasonal number of days of soil moisture deficit by 2090 for RCP4.5.	46
Figure 8-9: Projected change in annual number of days of soil moisture deficit by 2090 for RCP8.5.	47
Figure 8-10: Projected change in seasonal number of days of soil moisture deficit by 2090 for RCP8.5.	48
Figure 9-1: Land classes of Tasman District.	50
Figure 11-1: Schematic showing dynamical downscaling method used in this report.	56
Figure 11-2: CMIP5 multi-model simulated time series from 1950-2100 for change in global annual mean surface temperature relative to 1986-2005.	58

Executive summary

This report provides climate change projections for six climate variables for Tasman District, which are additional to those presented in the 2015 NIWA climate change report for the region. The variables are heatwave days, growing degree days, heavy rain days, extreme rainfall, potential evapotranspiration deficit (drought potential) and soil moisture deficit days.

The Tasman District will likely experience a warmer, wetter climate with increased seasonal climate extremes. Drought intensity may increase in the summer and heavy rainfall may increase in the winter and spring. Ex-tropical cyclones will continue to affect the region from time to time, and the rainfall intensity from those systems may increase. Frost incidence is likely to fall, and the occurrence of high temperatures and heatwaves will increase.

Information about potential impacts of climate change on agricultural systems in Tasman was requested to inform changes to the Council's land classification system. Climate change is likely to have varying effects on agricultural systems in the region. The highly flexible land classes in coastal lowland areas such as Waimea Plains, around Motueka and Takaka, and in valleys further inland, are already the warmest parts of the region and will become warmer in the future. This may have impacts on the land uses and crop types that are currently grown in these areas due to changes to plant development rates and heat stress. For less flexible land (e.g. around Motupiko, Lake Rotoiti and Bainham), if these areas are limited by cold conditions rather than other factors such as soil type and topography, future warming presents an opportunity for these areas to become more flexible. Increasing drought intensity across the region, but particularly in central areas, in summer may impact pasture and crop growth and increase the need for irrigation, as well as increasing fire risk in forested areas. Winter rainfall in particular is projected to increase, and extreme rainfall events may increase in intensity, potentially causing more slips on hill country farmland and deforested areas.

1 Introduction

Tasman District Council (TDC) requested climate change advice from NIWA under two Envirolink small advice grants (1974-TSDC157 and 1975-TDSC158). For ease of use of this information, these two small advice grants have been combined into one report. This report provides information about climate change projections further to the NIWA climate change and variability report provided to TDC in 2015 (<https://www.tasman.govt.nz/my-region/civil-defence/climate-change/>). Climate variables which have been extracted from the regional climate model since 2015, presented here, include heatwave days, growing degree days, heavy rain days (>25 mm), potential evapotranspiration deficit (a measure of drought potential), and soil moisture deficit. In addition, a sixth variable, extreme rainfall, has been extracted from NIWA's High Intensity Rainfall Design System (HIRDS v4). These variables are presented as maps or tables for two climate change scenarios (Representative Concentration Pathways) and two future time periods (2040 and 2090).

The climate change maps and a productive land classification map for Tasman was used to understand potential climate change impacts on productive land and agricultural systems in the Tasman District.

2 Methodology

The following bullet points summarise the methodology used by NIWA for modelling New Zealand's future climate. More details about the methods and the Representative Concentration Pathways are found in Appendix A and B.

- Climate model simulation data from the IPCC Fifth Assessment has been used to produce climate projections for New Zealand.
- Six climate models were chosen by NIWA for dynamical downscaling. These models were chosen because they produced the most accurate results when compared to historical climate and circulation patterns in the New Zealand and southwest Pacific region.
- Downscaled climate change projections are at a 5 km x 5 km resolution over New Zealand.
- Climate projection and historic baseline maps and tables present the average of the six downscaled models.
- Climate projections are presented as a 20-year average for two future periods: 2031-2050 (termed '2040') and 2081-2100 (termed '2090'). All maps show changes relative to the baseline climate of 1986-2005 (termed '1995').
- Two Representative Concentration Pathways (RCPs) are presented, RCP4.5 (a mid-range scenario) and RCP8.5 (the 'business as usual' scenario).

3 Heatwave day projections

The definition of a heatwave considered here is a period of three or more consecutive days where the maximum daily temperature exceeds 25°C. This calculation is an aggregation of all days per year that are included in a heatwave (i.e., \geq three consecutive days with maximum temperature $> 25^\circ\text{C}$), no matter the length of the heatwave. The annual heatwave days are then averaged over the 20-year period of interest (e.g., 2031-2050) to get the average annual heatwave-day climatology (past) and future projections.

Historic (average over 1986-2005) and future (average over 2031-2050 and 2081-2100) maps for heatwave days are shown in this section. The historic maps show annual average numbers of heatwave days and the future maps show both the change in the annual number of heatwave days compared with the historic period and the total future number of heatwave days.

For the historic period, the southern valleys of Tasman District around Murchison, as well as the Waimea Plains, observe the most heatwave days per year (10-15 days per year) (Figure 3-1). Other low-lying inland valleys, as well as around Takaka and Motueka, observe 6-8 heatwave days per year.

In the future, the number of heatwave days is projected to increase, particularly in locations where the historic number of heatwave days is high (e.g. southern valleys, Waimea Plains, etc.) (Figure 3-2). By 2040 for both RCP4.5 and RCP8.5, increases of 10-15 heatwave days per year are projected for the southern valleys. 5-10 more heatwave days per year are projected for most other lowland or foothill parts of the region. By 2090 under RCP4.5, 20-25 more heatwave days are projected for the southern valleys, and 10-20 more heatwave days are projected for most other lowland and foothill areas. However, there is a significant increase in heatwave days under RCP8.5 by 2090, with >50 more heatwave days per year projected for the southern valleys and a small part of the Waimea Plains near Appleby. Increases of 30-50 more heatwave days per year are projected for most other lowland and foothill areas. As another way of presenting the information, Figure 3-3 presents the total number of heatwave days projected under both scenarios at both future time periods.

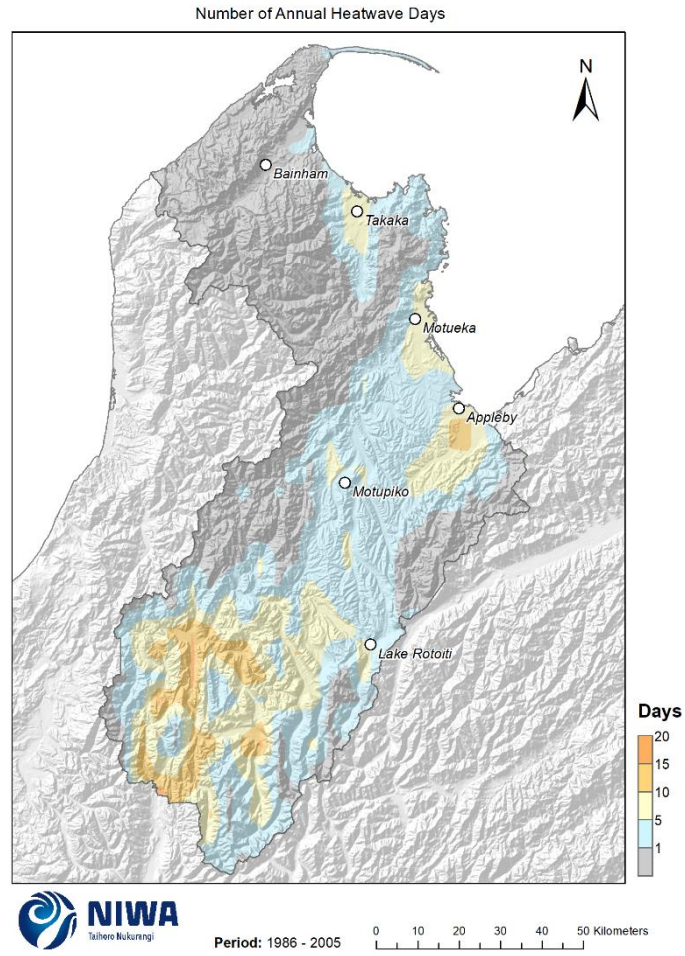


Figure 3-1: Modelled annual number of heatwave days (≥ three consecutive days with maximum temperatures > 25°C), average over the historic period 1986-2005. Results are based on dynamical downscaled projections using NIWA's Regional Climate Model. Resolution of projection is 5km x 5km.

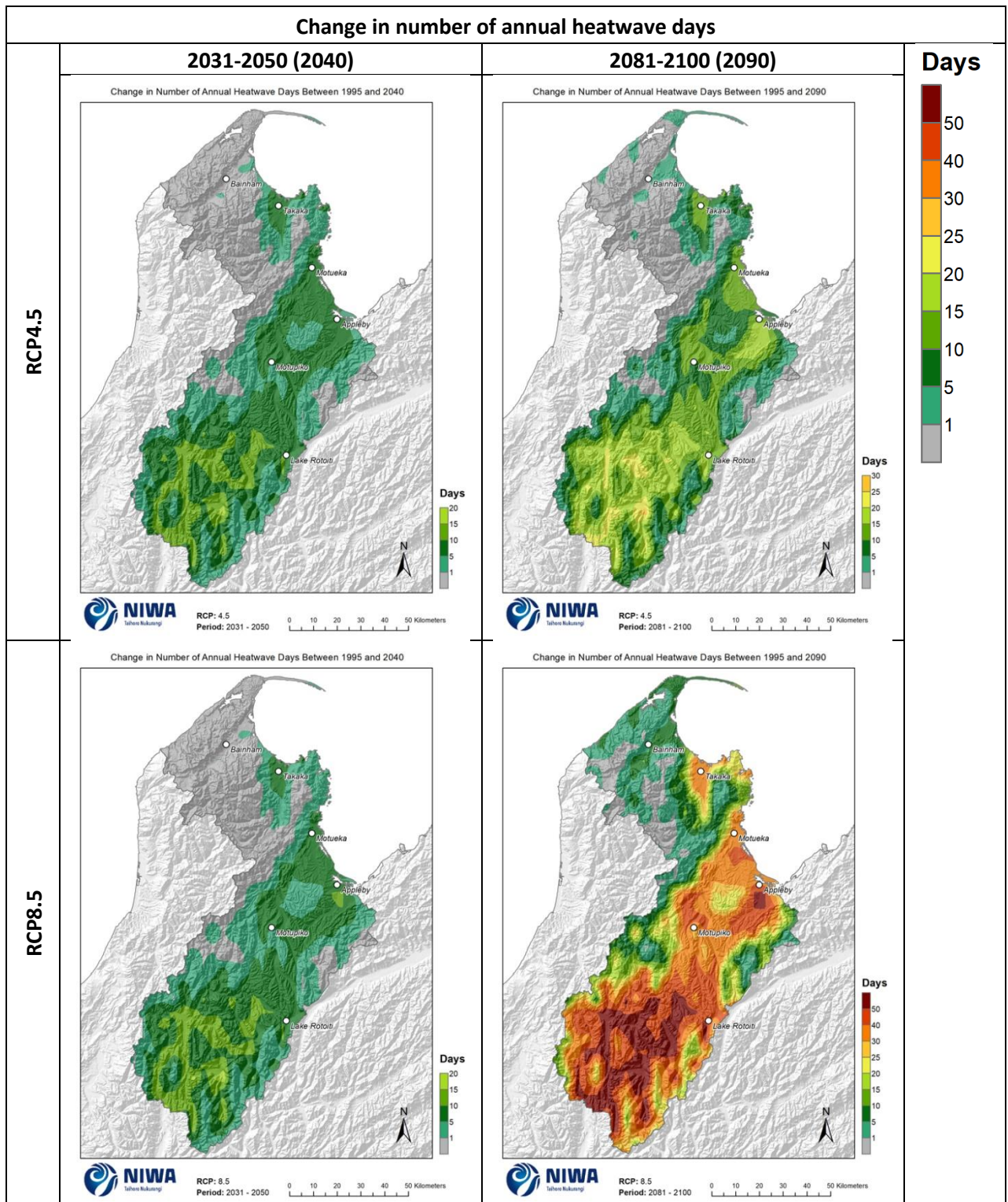


Figure 3-2: Projected annual heatwave day changes (number of days within periods of \geq three consecutive days with maximum temperatures $> 25^\circ\text{C}$) at 2040 and 2090. Relative to 1986-2005 average, for RCP4.5 and RCP8.5, based on the average of six global climate models. Results are based on dynamical downscaled projections using NIWA's Regional Climate Model. Resolution of projection is 5km x 5km.

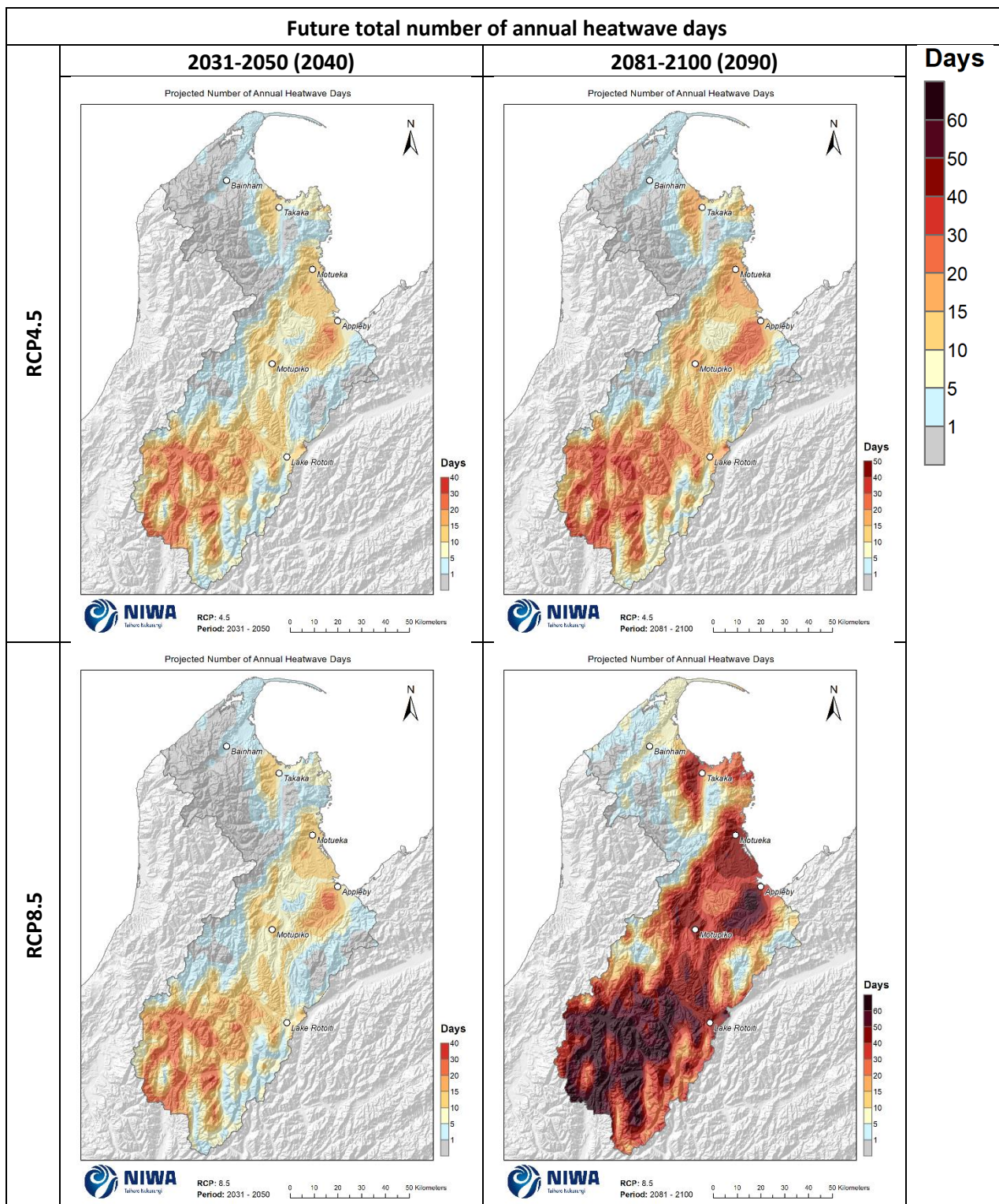


Figure 3-3: Projected annual total number of heatwave days (number of days within periods of \geq three consecutive days with maximum temperatures $> 25^{\circ}\text{C}$) at 2040 and 2090. For RCP4.5 and RCP8.5, based on the average of six global climate models. Results are based on dynamical downscaled projections using NIWA's Regional Climate Model. Resolution of projection is 5km x 5km.

4 Growing degree day projections

Growing degree-days (GDD) express the sum of daily temperatures above a selected base temperature (e.g. 10°C) that represent a threshold for plant growth. The average amount of GDD in a location may influence the choice of crops to grow, as different species have different temperature thresholds for survival. The daily GDD total is the amount the daily average temperature exceeds the threshold value (e.g. 10°C) per day. For example, a daily average temperature of 18°C would have a GDD base 10°C value of 8. Here, GDD are accumulated from July to June, and presented for the historic period (average over 1986-2005) and future change (average over 2031-2050 and 2081-2100).

Historic (average over 1986-2005) and future (average over 2031-2050 and 2081-2100) maps for GDD are shown in this section for a base temperature of 10°C. The historic maps show annual average numbers of GDD and the future projection maps show the both the change in the annual number of GDD compared with historic and the total future numbers of GDD.

For the historic period, the highest number of GDD is experienced in low-lying coastal areas around the region, including Takaka, Golden Bay, and Tasman Bay from Motueka to Appleby and including the Waimea Plains (1200-1400 GDD per year) (Figure 4-1). Numbers of GDD experienced generally decline further inland, with 1000-1200 GDD experienced near Bainham and Motupiko, and 600-800 GDD per year at Lake Rotoiti. Conversely, higher GDD is experienced around the southern valleys near Murchison, with 800-1200 GDD per year. High elevations experience up to 400 GDD per year.

In the future, GDD in Tasman is projected to increase under both scenarios (Figure 4-2). By 2040 under RCP4.5, most of the region is likely to experience increases of 150-200 GDD per year, on average (higher elevations expect smaller increases of 50-150 GDD per year). Under RCP8.5 by 2040, key areas around Takaka, Motueka, Appleby, Waimea Plains, Tasman Bay, Motupiko and the southern valleys are projected to experience 200-250 more GDD per year. By 2090, under RCP4.5, increases of 250-300 GDD per year are likely for most locations, with larger increases of 300-400 GDD projected for the Waimea Plains and the southern valleys. Under RCP8.5 there is a significant increase in GDD projected for the whole region, with the most being 700-800 more GDD for the southern valleys, 600-700 more GDD for much of the region inland from Tasman Bay as well as around Takaka, and 500-600 more GDD for other foothill areas. As another way of presenting the information, Figure 4-3 presents the total number of growing degree days projected under both scenarios at both future time periods.

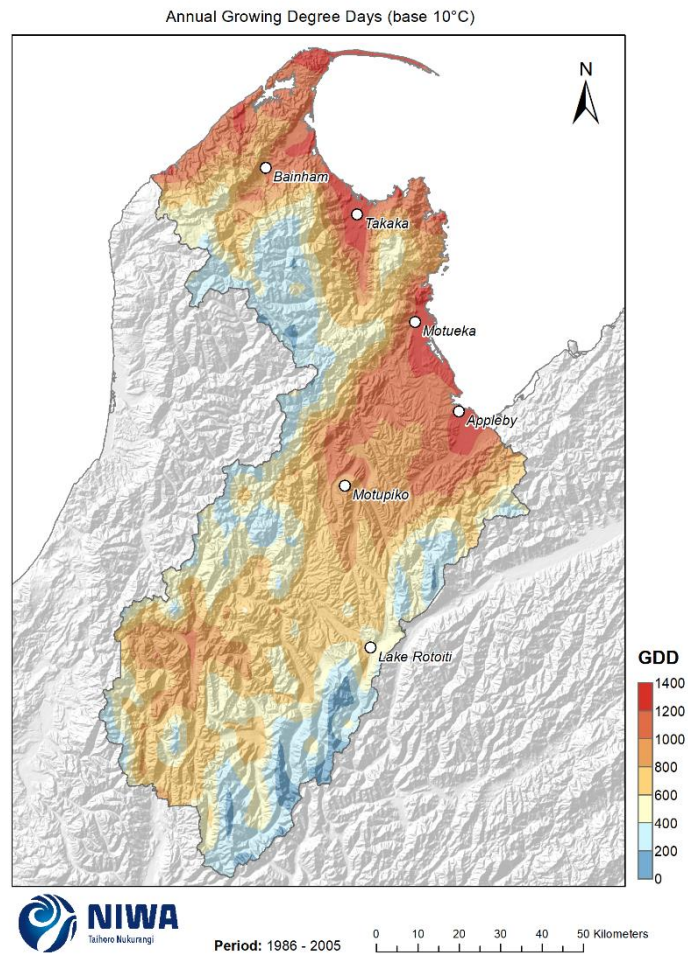


Figure 4-1: Modelled annual number of growing degree days (base 10°C), average over the historic period 1986-2005. Results are based on dynamical downscaled projections using NIWA's Regional Climate Model. Resolution of projection is 5km x 5km.

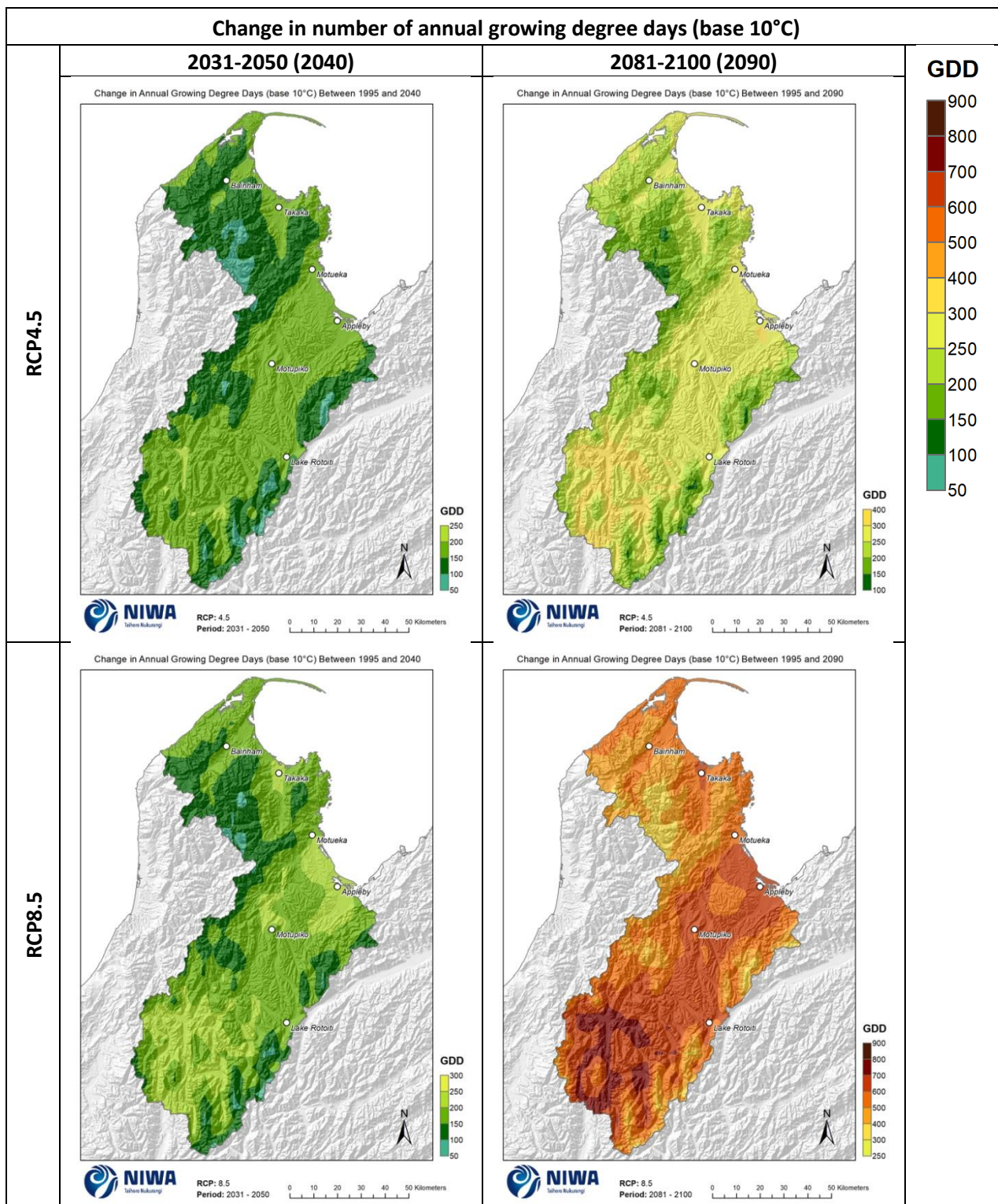


Figure 4-2: Projected annual growing degree day changes (base 10°C) at 2040 and 2090. Relative to 1986-2005 average, for RCP4.5 and RCP8.5, based on the average of six global climate models. Results are based on dynamical downscaled projections using NIWA's Regional Climate Model. Resolution of projection is 5km x 5km.

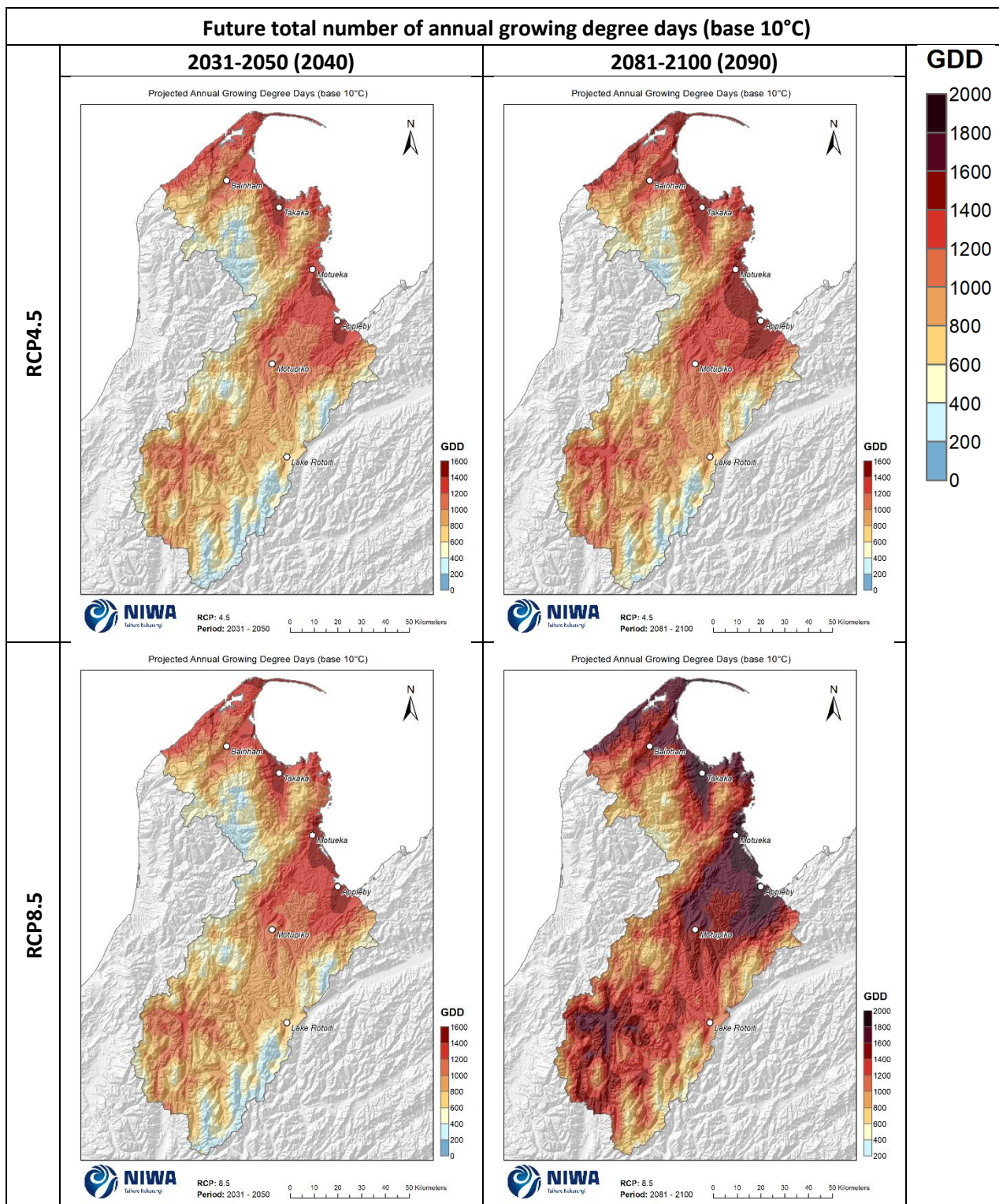


Figure 4-3: Projected total number of annual growing degree days (base 10°C) at 2040 and 2090. For RCP4.5 and RCP8.5, based on the average of six global climate models. Results are based on dynamical downscaled projections using NIWA's Regional Climate Model. Resolution of projection is 5km x 5km.

5 Heavy rain day projections (> 25 mm)

A heavy rain day considered here is a daily rainfall total above 25 mm. Historic (average over 1986-2005) and future (average over 2031-2050 and 2081-2100) maps for heavy rain days are shown in this section. The historic maps show annual and seasonal average numbers of heavy rain days and the future projection maps show the change in the number of heavy rain days compared with the historic period. Note that the historic maps are on a different colour scale to the future projection maps.

For the historic period, the greatest number of heavy rain days occurs in the Tasman Mountains (80-100 days per year) (Figure 5-1). The least heavy rain days occurs inland from Tasman Bay to Motupiko (5-10 days per year). Most of the region experiences 15-40 heavy rain days per year. By season (Figure 5-2), most rain days occur in spring and the least occur in summer.

Future projections are shown in Figure 5-3 to Figure 5-10. By 2040, the annual number of heavy rain days is projected to increase by 0-2 days per year across most of the region under both scenarios, and 2-3 more heavy rain days projected for western and southern areas under RCP8.5. Small decreases (0-1 day per year) are projected for the high elevations of the Tasman Mountains. By 2090, the projections are similar to 2040 for RCP4.5 but changes are more substantial for RCP8.5. For the southern part of the region, increases of 4-6 heavy rain days per year are projected and increases of 2-4 days likely for most of the rest of the region. Decreases of 0-2 days per year are projected for the Tasman Mountains. The largest reductions in heavy rain days are projected for summer and the largest increases are projected for winter and spring.

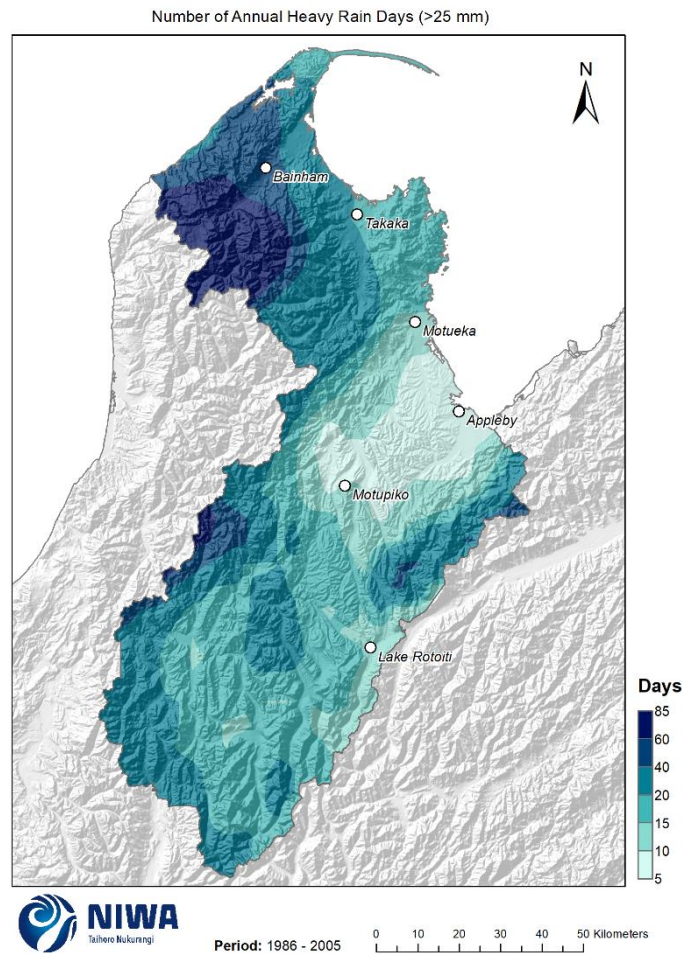


Figure 5-1: Modelled annual number of heavy rain days (>25mm) (average over the historic period 1986-2005). Based on the average of six global climate models. Results are based on dynamical downscaled projections using NIWA's Regional Climate Model. Resolution of projection is 5km x 5km.

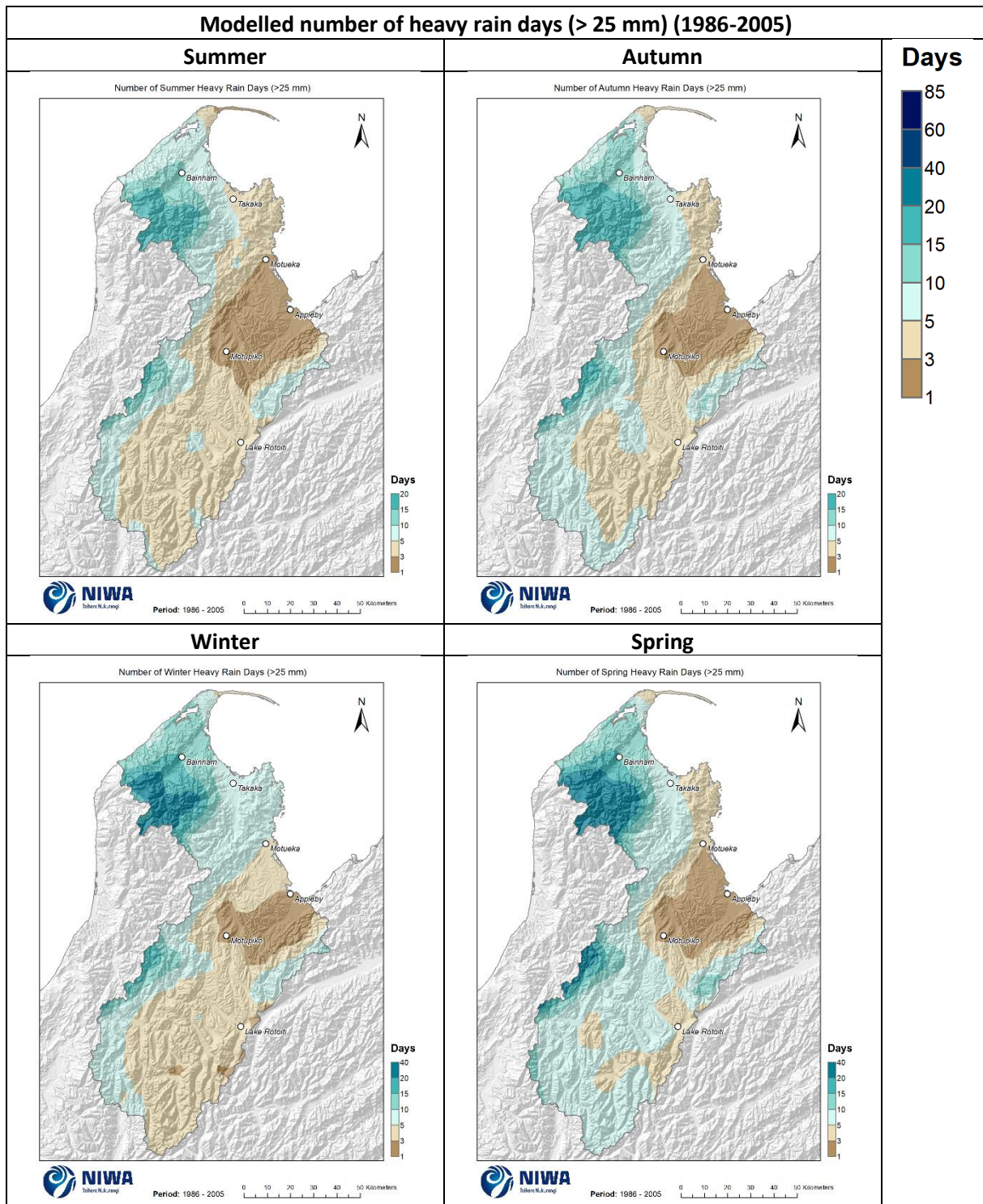


Figure 5-2: Modelled seasonal number of heavy rain days (>25mm) (average over the historic period 1986-2005). Based on the average of six global climate models. Results are based on dynamical downscaled projections using NIWA's Regional Climate Model. Resolution of projection is 5km x 5km.

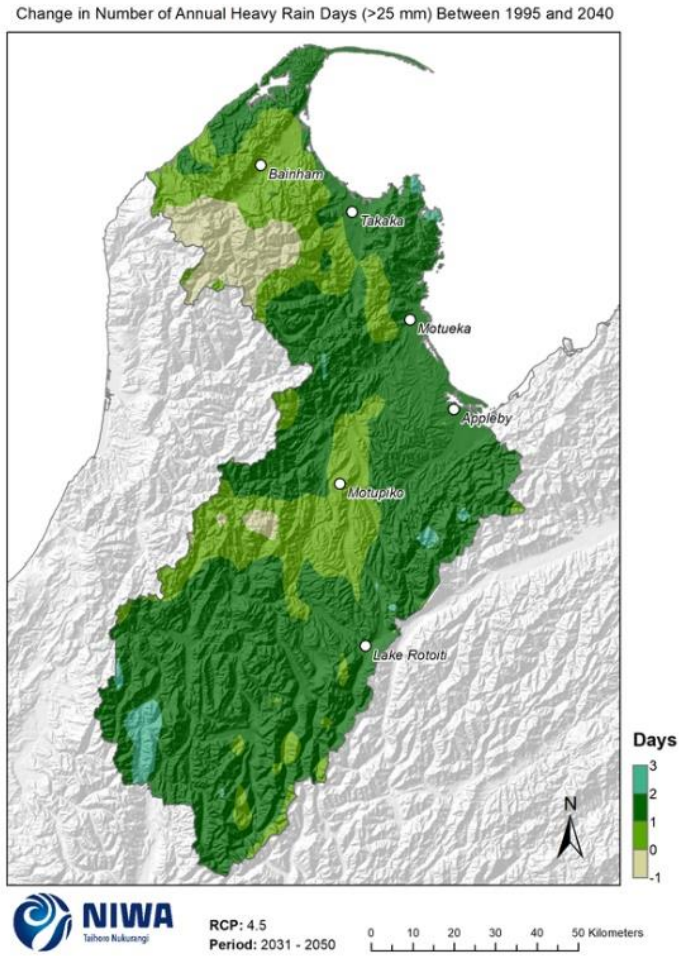


Figure 5-3: Projected change in annual number of heavy rain days (>25mm) by 2040 for RCP4.5. Relative to 1986-2005 average, based on the average of six global climate models. Results are based on dynamical downscaled projections using NIWA's Regional Climate Model. Resolution of projection is 5km x 5km.

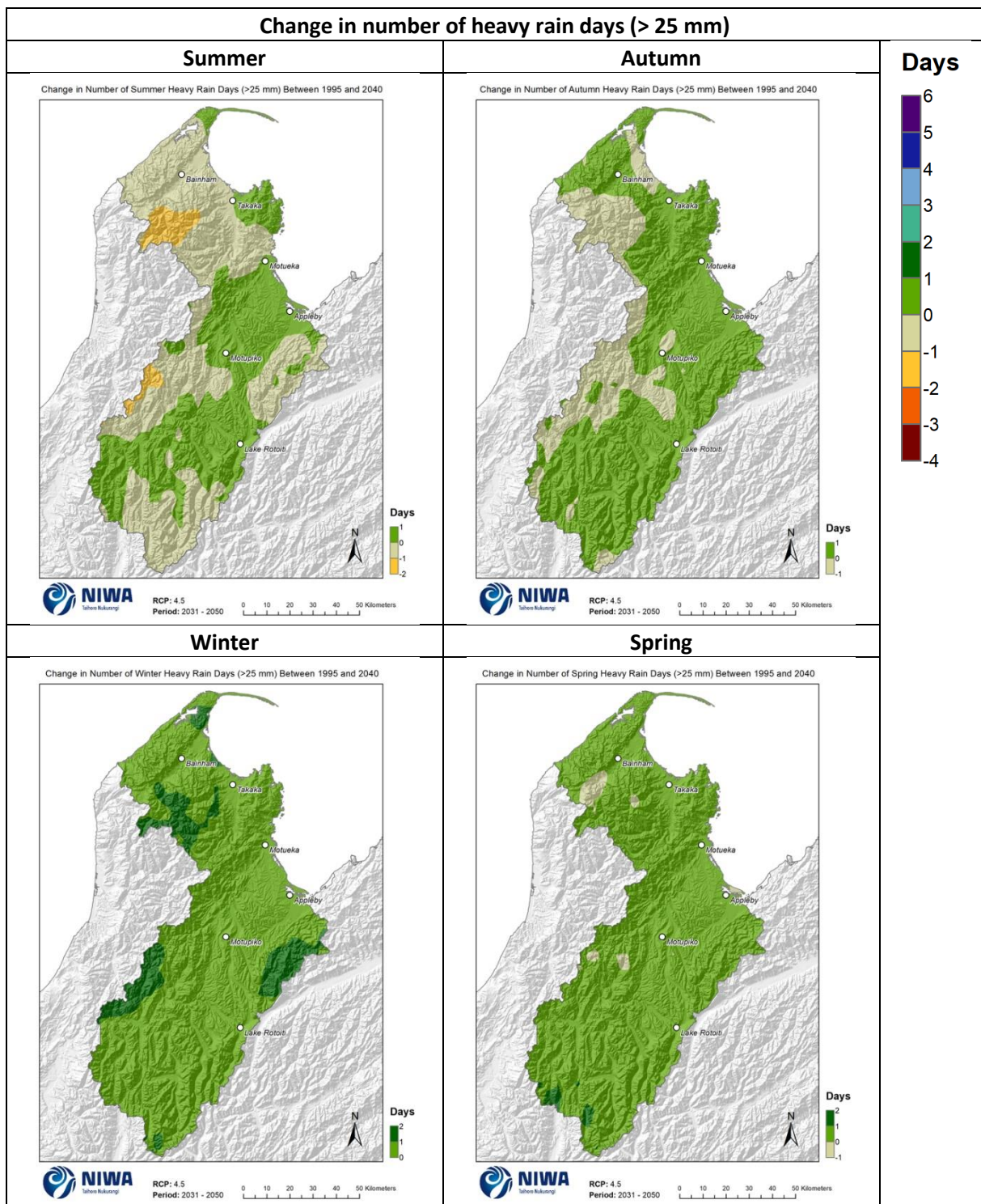


Figure 5-4: Projected change in seasonal number of heavy rain days (>25mm) by 2040 for RCP4.5. Relative to 1986-2005 average, based on the average of six global climate models. Results are based on dynamical downscaled projections using NIWA's Regional Climate Model. Resolution of projection is 5km x 5km.

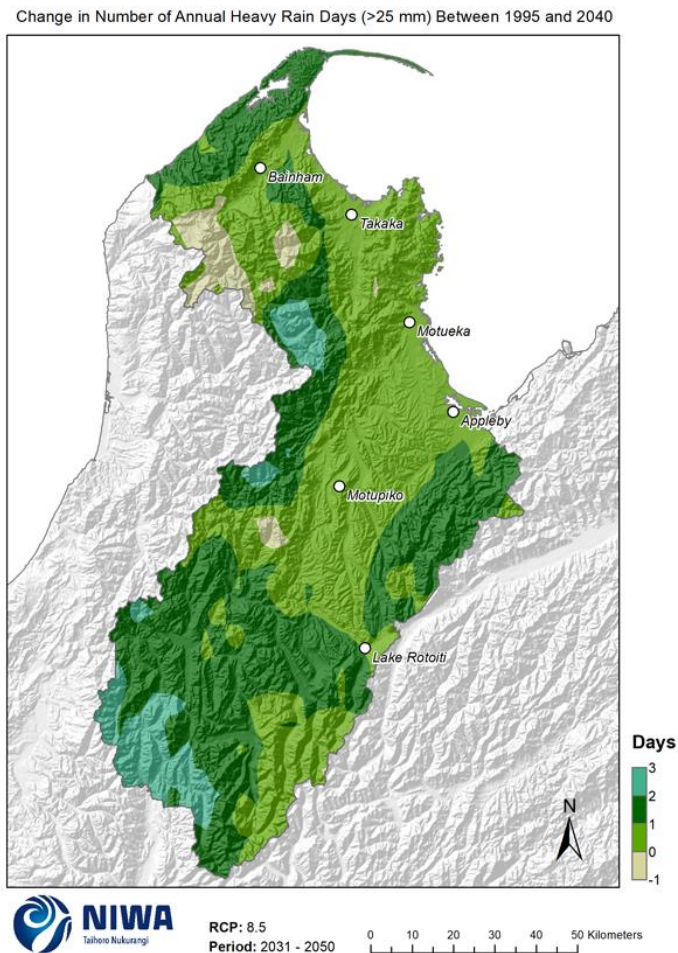


Figure 5-5: Projected change in annual number of heavy rain days (>25mm) by 2040 for RCP8.5. Relative to 1986-2005 average, based on the average of six global climate models. Results are based on dynamical downscaled projections using NIWA's Regional Climate Model. Resolution of projection is 5km x 5km.

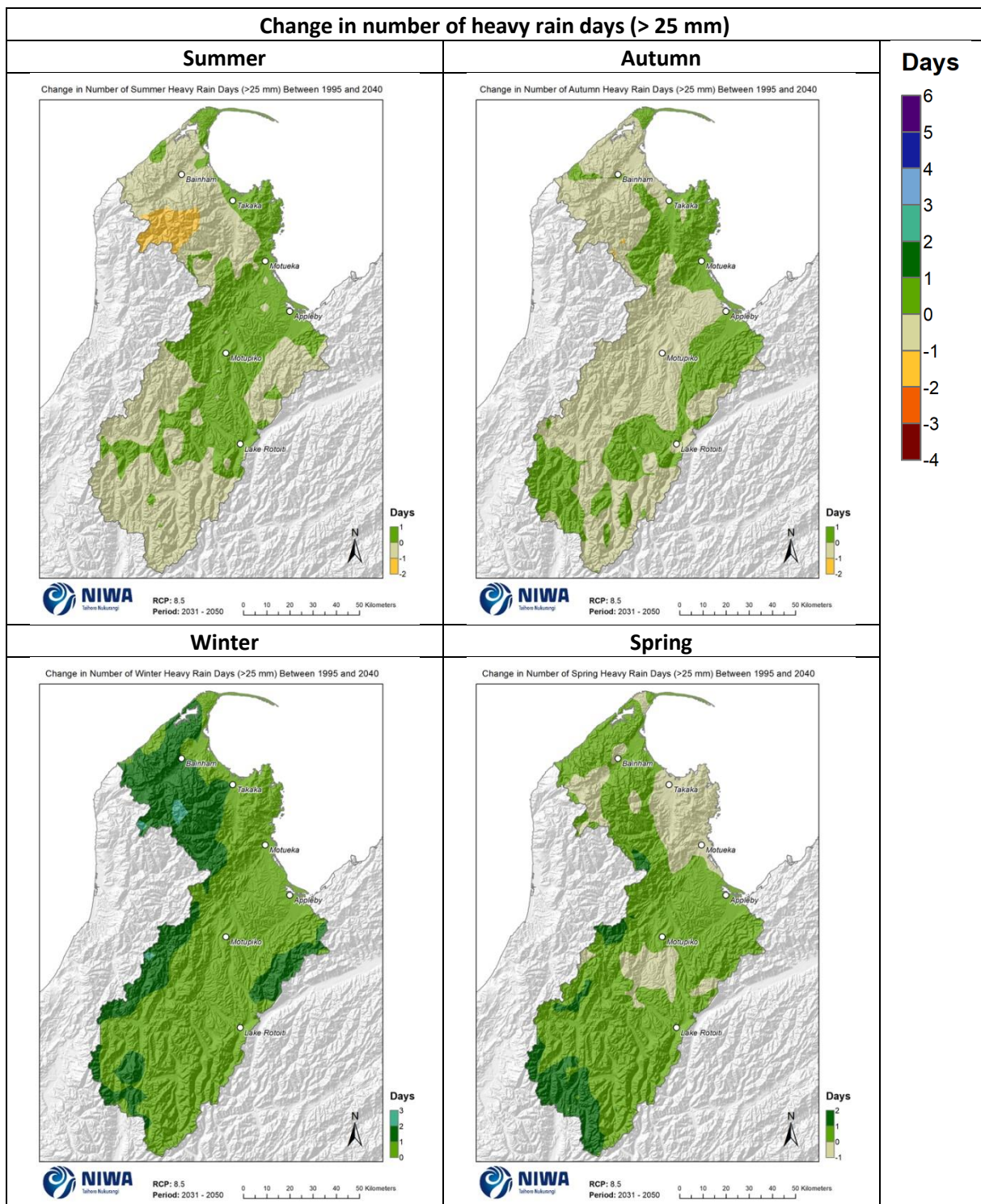


Figure 5-6: Projected change in seasonal number of heavy rain days (>25mm) by 2040 for RCP8.5. Relative to 1986-2005 average, based on the average of six global climate models. Results are based on dynamical downscaled projections using NIWA's Regional Climate Model. Resolution of projection is 5km x 5km.

Change in Number of Annual Heavy Rain Days (>25 mm) Between 1995 and 2090

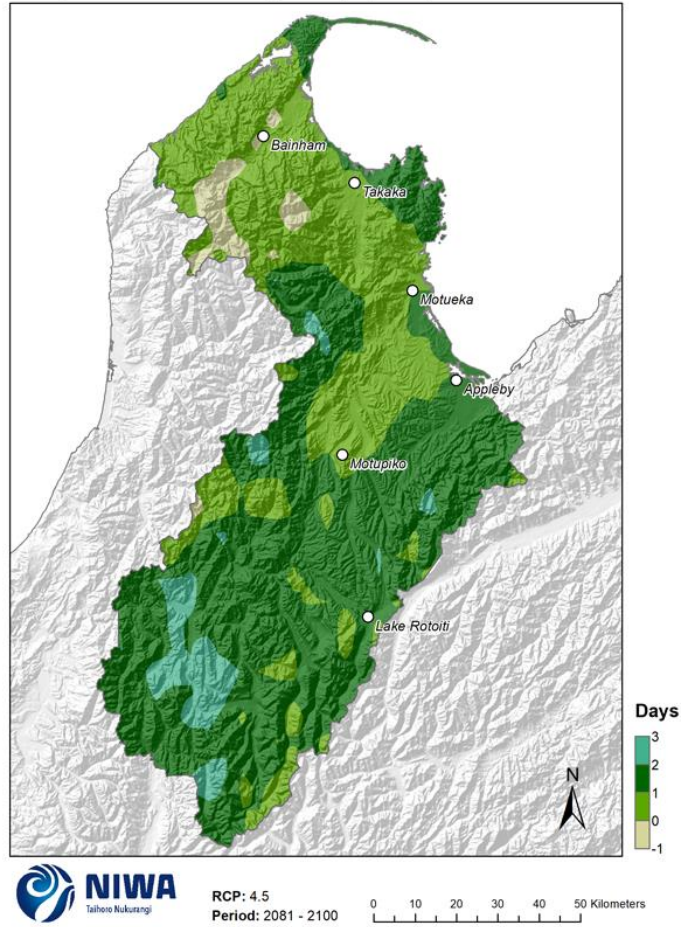


Figure 5-7: Projected change in annual number of heavy rain days (>25mm) by 2090 for RCP4.5. Relative to 1986-2005 average, based on the average of six global climate models. Results are based on dynamical downscaled projections using NIWA's Regional Climate Model. Resolution of projection is 5km x 5km.

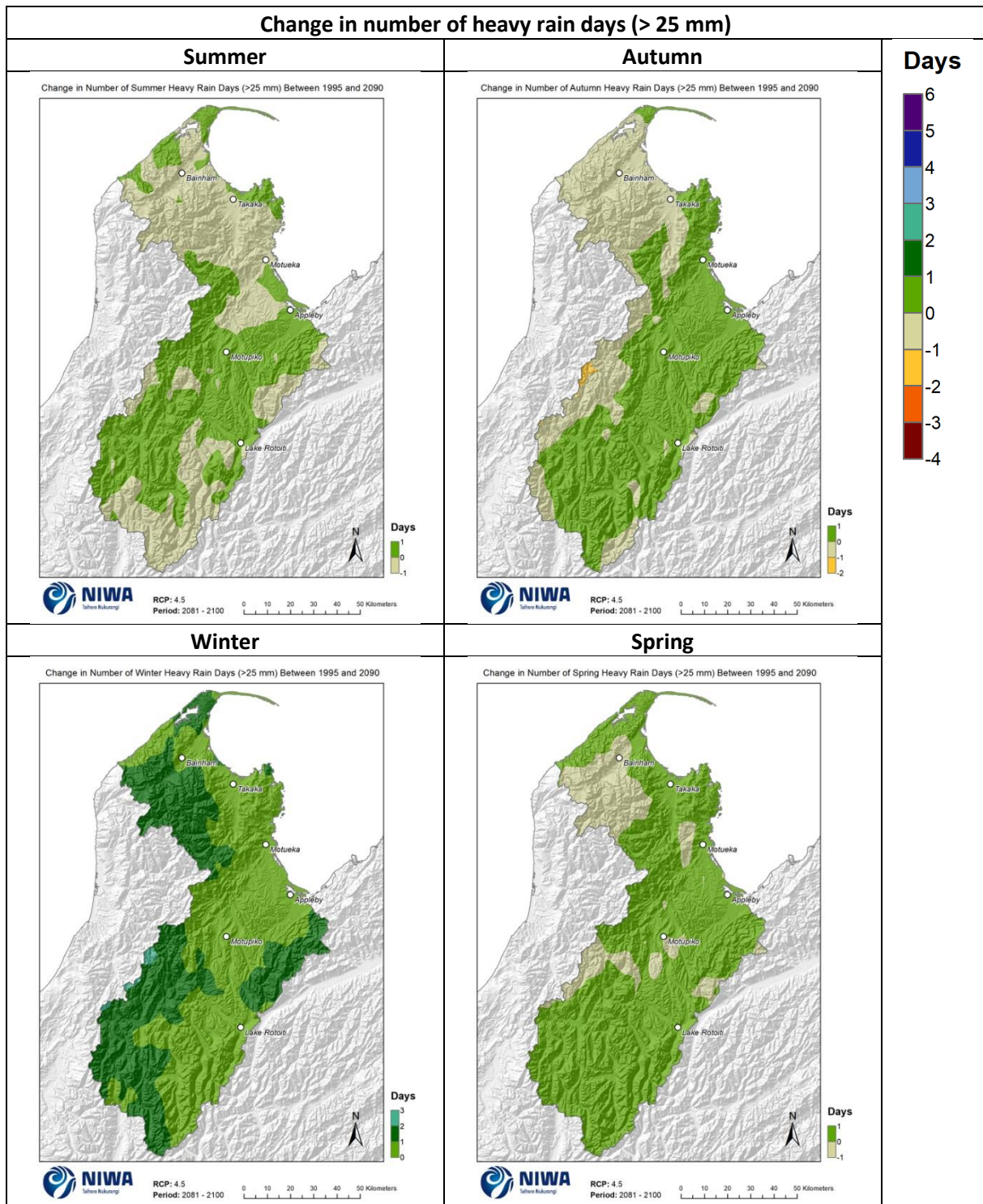


Figure 5-8: Projected change in seasonal number of heavy rain days (>25mm) by 2090 for RCP4.5. Relative to 1986-2005 average, based on the average of six global climate models. Results are based on dynamical downscaled projections using NIWA's Regional Climate Model. Resolution of projection is 5km x 5km.

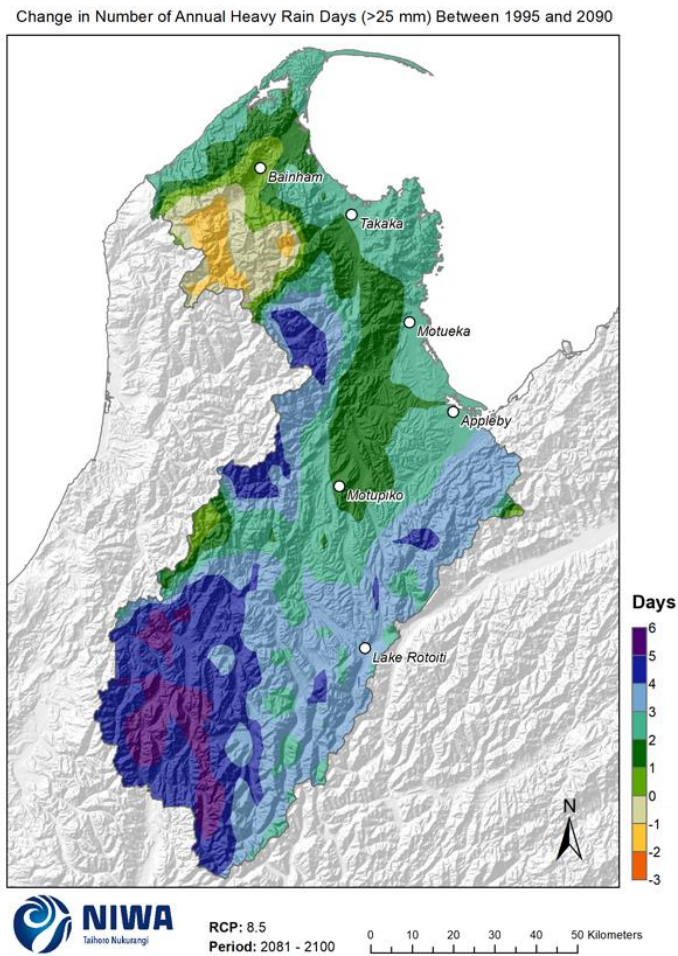


Figure 5-9: Projected change in annual number of heavy rain days (>25mm) by 2090 for RCP8.5. Relative to 1986-2005 average, based on the average of six global climate models. Results are based on dynamical downscaled projections using NIWA's Regional Climate Model. Resolution of projection is 5km x 5km.

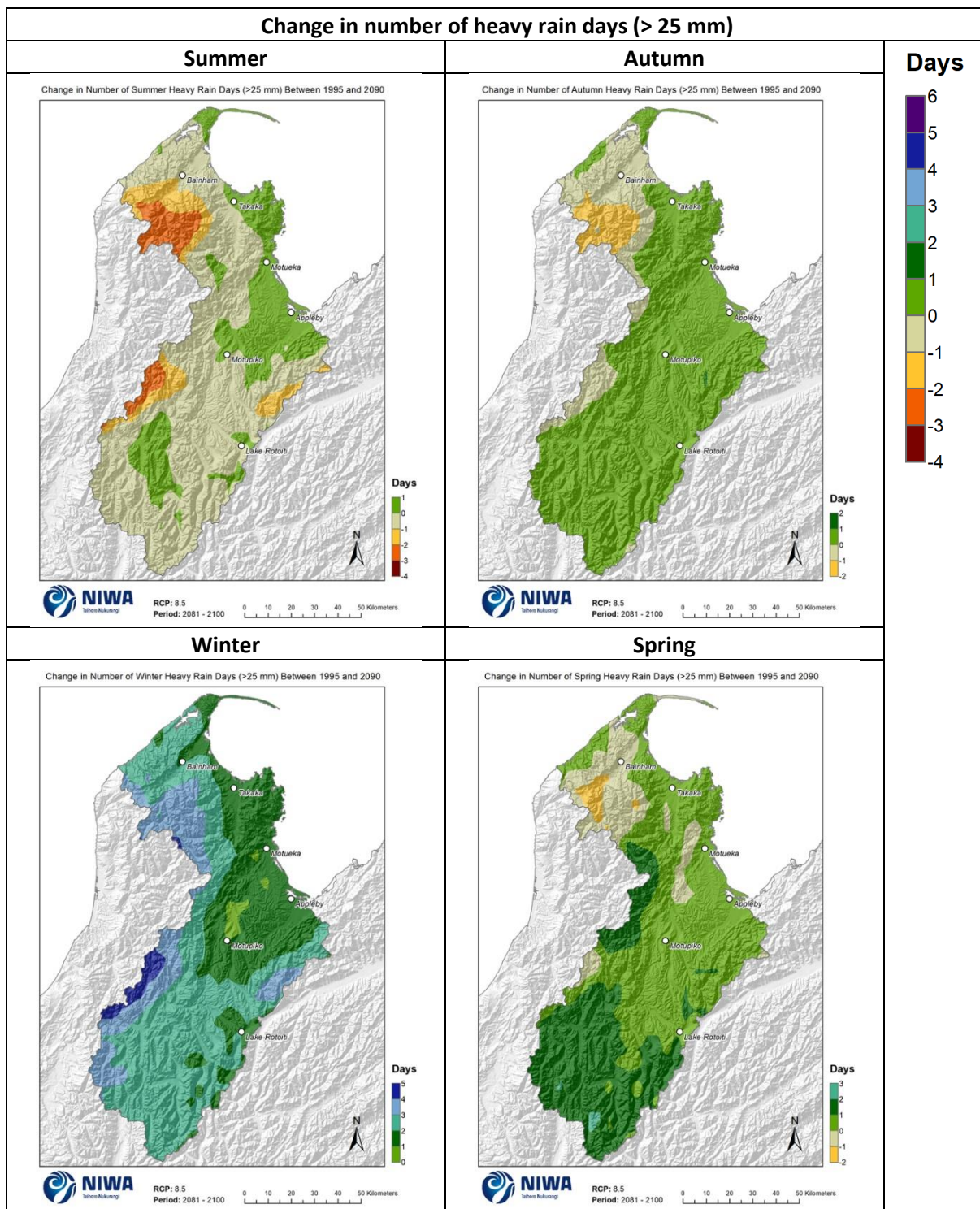


Figure 5-10: Projected change in seasonal number of heavy rain days (>25mm) by 2090 for RCP8.5. Relative to 1986-2005 average, based on the average of six global climate models. Results are based on dynamical downscaled projections using NIWA's Regional Climate Model. Resolution of projection is 5km x 5km.

6 Extreme rainfall projections (HIRDS v4)

Extreme, rare rainfall events may cause significant damage to land, buildings, and infrastructure. This section analyses how these rainfall events may change in the future for Tasman.

Extreme rainfall events (and floods) are often considered in the context of return periods (e.g. 1-in-100-year rainfall events). A return period, also known as a recurrence interval, is an estimate of the likelihood of an event. It is a statistical measure typically based on historic data and probability distributions which calculate how often an event of a certain magnitude may occur. Return periods are often used in risk analysis and infrastructure design.

The theoretical return period is the inverse of the probability that the event will be exceeded in any one year. For example, a 1-in-10-year rainfall event has a $1/10 = 0.1$ or 10% chance of being exceeded in any one year and a 1-in-100-year rainfall event has a $1/100 = 0.01$ or 1% chance of being exceeded in any one year. However, this does not mean that a 1-in-100-year rainfall event will happen regularly every 100 years, or only once in 100 years. The events with larger return periods (i.e. 1-in-100-year events) have larger rainfall amounts for the same duration as events with smaller return periods (i.e. 1-in-2-year events) because larger events occur less frequently (on average).

A warmer atmosphere can hold more moisture, so there is potential for heavier extreme rainfall with global increases in temperatures under climate change (Fischer and Knutti, 2016, Trenberth, 1999). The frequency of heavy rainfall events is 'very likely' to increase over most mid-latitude land areas (this includes New Zealand; IPCC, 2013). Given the mountainous nature of New Zealand, spatial patterns of changes in rainfall extremes are expected to depend on changes in atmospheric circulation and storm tracks.

NIWA's High Intensity Rainfall Design System (HIRDS) allows rainfall event recurrence intervals to be calculated for any location in New Zealand. HIRDS calculates historic recurrence intervals as well as future potential recurrence intervals based on climate change scenarios. The 2018 HIRDS version 4 (Carey-Smith et al., 2018) updated the scenarios to those presented in this report (i.e. the IPCC's Fifth Assessment Report scenarios). The future rainfall increases calculated by the HIRDS v4 tool are based on a percent change per degree of warming. The short duration, rare events have the largest relative increases of around 14%, while the longest duration events increase by about 5 to 6%. HIRDS v4 can be freely accessed at www.hirds.niwa.co.nz, and more background information to the HIRDS methodology can be found at <https://www.niwa.co.nz/information-services/hirds/help>.

HIRDS rainfall projections for locations in the Tasman District (Figure 6-1) are presented in Table 6-1 to Table 6-6. These tables show the historic rainfall depths per duration and return period (ARI, average recurrence interval, and AEP, annual exceedance probability), as well as future projections for RCP4.5 and RCP8.5 by 2040 and 2090, for each location in Figure 6-1.



Figure 6-1: Locations/station network numbers for HIRDS rainfall analysis.

Table 6-1: Extreme rainfall projections for Bainham, from HIRDS v4.

Site name	Bainham												
Site ID	F02751												
Rainfall depths (mm) :: Historical Data													
ARI	AEP	10m	20m	30m	1h	2h	6h	12h	24h	48h	72h	96h	120h
2	0.5	7.66	13.7	18.9	31.6	50.4	96	136	184	237	269	292	310
5	0.2	9.92	17.8	24.5	40.8	65	124	175	236	304	345	374	396
10	0.1	11.6	20.8	28.6	47.7	75.9	144	203	274	353	401	435	460
20	0.05	13.4	23.9	32.9	54.8	87.1	165	233	314	404	458	497	526
50	0.02	15.8	28.3	38.9	64.6	103	194	274	368	473	537	581	615
100	0.01	17.7	31.6	43.5	72.2	115	217	305	410	527	597	647	684
Rainfall depths (mm) :: RCP4.5 for the period 2031-2050													
ARI	AEP	10m	20m	30m	1h	2h	6h	12h	24h	48h	72h	96h	120h
2	0.5	8.35	15	20.7	34.5	54.7	103	144	193	248	280	303	321
5	0.2	10.9	19.5	26.8	44.7	70.9	133	187	249	319	361	390	412
10	0.1	12.7	22.8	31.4	52.3	82.9	156	218	291	372	420	454	480
20	0.05	14.7	26.3	36.2	60.2	95.3	179	250	333	426	481	519	548
50	0.02	17.4	31.1	42.7	71	112	210	294	391	499	564	609	642
100	0.01	19.5	34.8	47.9	79.5	126	235	328	436	556	628	678	715
Rainfall depths (mm) :: RCP4.5 for the period 2081-2100													
ARI	AEP	10m	20m	30m	1h	2h	6h	12h	24h	48h	72h	96h	120h
2	0.5	8.79	15.8	21.7	36.3	57.5	107	150	200	255	287	310	328
5	0.2	11.5	20.5	28.3	47.1	74.7	139	194	258	329	371	400	422
10	0.1	13.5	24.1	33.2	55.3	87.4	163	227	301	383	433	466	492
20	0.05	15.5	27.8	38.2	63.6	101	187	260	345	439	495	534	562
50	0.02	18.4	32.9	45.2	75.1	119	221	306	406	516	581	626	660
100	0.01	20.6	36.9	50.6	84.1	133	247	342	453	575	647	697	734
Rainfall depths (mm) :: RCP8.5 for the period 2031-2050													
ARI	AEP	10m	20m	30m	1h	2h	6h	12h	24h	48h	72h	96h	120h
2	0.5	8.45	15.2	20.9	34.9	55.4	104	146	195	249	282	305	322
5	0.2	11	19.7	27.2	45.3	71.8	135	188	251	321	363	392	414
10	0.1	12.9	23.1	31.8	53	84	157	220	293	374	423	457	482
20	0.05	14.9	26.6	36.7	61	96.5	181	252	336	429	484	523	552
50	0.02	17.6	31.5	43.3	72	114	213	297	394	503	568	613	646
100	0.01	19.8	35.3	48.5	80.6	127	238	331	440	561	632	682	719
Rainfall depths (mm) :: RCP8.5 for the period 2081-2100													
ARI	AEP	10m	20m	30m	1h	2h	6h	12h	24h	48h	72h	96h	120h
2	0.5	10.1	18.1	24.9	41.6	65.6	120	166	218	274	308	331	348
5	0.2	13.2	23.7	32.6	54.3	85.6	157	216	283	356	400	429	451
10	0.1	15.5	27.8	38.3	63.8	101	184	253	332	417	468	502	528
20	0.05	18	32.1	44.2	73.6	116	212	291	380	479	536	576	604
50	0.02	21.3	38.1	52.4	87.1	137	251	343	448	564	631	677	710
100	0.01	23.9	42.7	58.8	97.6	153	281	384	501	629	704	755	792

Table 6-2: Extreme rainfall projections for Takaka, from HIRDS v4.

Site name	Takaka												
Site ID	F02885												
Rainfall depths (mm) :: Historical Data													
ARI	AEP	10m	20m	30m	1h	2h	6h	12h	24h	48h	72h	96h	120h
2	0.5	8.64	13.9	18.3	29.1	45.1	83.6	116	150	180	192	198	200
5	0.2	11.3	18.2	23.9	37.9	58.7	108	150	194	232	248	255	258
10	0.1	13.3	21.4	28.2	44.6	68.9	127	175	226	271	289	298	301
20	0.05	15.4	24.8	32.6	51.5	79.5	146	202	260	311	332	341	345
50	0.02	18.4	29.5	38.7	61.1	94.2	173	238	307	367	391	402	406
100	0.01	20.7	33.2	43.6	68.8	106	194	267	344	410	437	449	453
Rainfall depths (mm) :: RCP4.5 for the period 2031-2050													
ARI	AEP	10m	20m	30m	1h	2h	6h	12h	24h	48h	72h	96h	120h
2	0.5	9.42	15.2	20	31.7	49	89.7	123	158	188	200	205	207
5	0.2	12.4	19.9	26.2	41.5	64	117	160	205	244	259	266	268
10	0.1	14.6	23.5	30.9	48.9	75.3	137	187	240	285	303	311	313
20	0.05	16.9	27.2	35.8	56.6	87	158	216	276	328	349	357	359
50	0.02	20.2	32.4	42.6	67.3	103	188	256	326	387	411	421	424
100	0.01	22.8	36.5	48	75.7	116	211	287	366	433	460	471	473
Rainfall depths (mm) :: RCP4.5 for the period 2081-2100													
ARI	AEP	10m	20m	30m	1h	2h	6h	12h	24h	48h	72h	96h	120h
2	0.5	9.91	16	21.1	33.4	51.5	93.5	127	163	193	205	210	212
5	0.2	13	21	27.7	43.8	67.4	122	166	212	251	267	273	275
10	0.1	15.4	24.8	32.6	51.6	79.4	144	195	248	294	312	319	321
20	0.05	17.9	28.7	37.8	59.8	91.8	166	225	286	338	359	367	369
50	0.02	21.4	34.3	45.1	71.1	109	197	267	338	400	424	433	435
100	0.01	24.1	38.7	50.8	80.1	123	221	300	380	448	474	484	486
Rainfall depths (mm) :: RCP8.5 for the period 2031-2050													
ARI	AEP	10m	20m	30m	1h	2h	6h	12h	24h	48h	72h	96h	120h
2	0.5	9.53	15.4	20.3	32.1	49.6	90.6	124	159	189	201	207	208
5	0.2	12.5	20.1	26.5	42.1	64.8	118	161	206	245	261	267	270
10	0.1	14.8	23.8	31.3	49.5	76.2	139	189	242	287	305	313	315
20	0.05	17.2	27.5	36.3	57.3	88.1	160	218	278	330	351	359	362
50	0.02	20.5	32.8	43.2	68.2	105	190	258	329	390	414	424	426
100	0.01	23.1	37	48.7	76.7	118	213	290	369	437	463	474	476
Rainfall depths (mm) :: RCP8.5 for the period 2081-2100													
ARI	AEP	10m	20m	30m	1h	2h	6h	12h	24h	48h	72h	96h	120h
2	0.5	11.4	18.3	24.1	38.3	58.7	105	141	177	208	220	224	225
5	0.2	15	24.2	31.8	50.5	77.3	138	185	232	272	288	293	294
10	0.1	17.8	28.6	37.7	59.6	91.2	162	218	274	320	338	344	345
20	0.05	20.7	33.2	43.7	69.2	106	188	252	315	369	389	396	396
50	0.02	24.8	39.7	52.2	82.4	126	224	299	374	437	460	468	468
100	0.01	28	44.8	58.9	92.9	142	252	337	420	490	515	524	524

Table 6-3: Extreme rainfall projections for Motueka (Riwaka), from HIRDS v4.

Site name	Motueka Riwaka												
Site ID	G12191												
Rainfall depths (mm) :: Historical Data													
ARI	AEP	10m	20m	30m	1h	2h	6h	12h	24h	48h	72h	96h	120h
2	0.5	8.5	11.8	14.5	20.9	30.4	53.9	75	100	127	142	151	158
5	0.2	11.2	15.5	19.1	27.4	39.6	70	97.2	130	164	183	194	202
10	0.1	13.3	18.4	22.5	32.3	46.6	82.1	114	151	191	213	226	235
20	0.05	15.5	21.3	26.1	37.4	53.9	94.6	131	174	219	243	258	268
50	0.02	18.5	25.5	31.1	44.4	63.9	112	154	204	257	285	302	314
100	0.01	20.9	28.8	35.1	50	71.8	125	172	228	286	317	336	349
Rainfall depths (mm) :: RCP4.5 for the period 2031-2050													
ARI	AEP	10m	20m	30m	1h	2h	6h	12h	24h	48h	72h	96h	120h
2	0.5	9.27	12.9	15.8	22.8	33	57.8	79.7	106	133	148	157	163
5	0.2	12.3	17	20.9	30	43.3	75.5	104	137	172	191	203	210
10	0.1	14.6	20.1	24.7	35.4	51	88.6	122	160	201	223	236	245
20	0.05	17	23.4	28.7	41	59	102	140	184	231	255	270	280
50	0.02	20.4	28	34.2	48.9	70.1	121	165	217	271	299	317	328
100	0.01	23.1	31.7	38.6	55.1	78.8	136	185	242	302	333	352	364
Rainfall depths (mm) :: RCP4.5 for the period 2081-2100													
ARI	AEP	10m	20m	30m	1h	2h	6h	12h	24h	48h	72h	96h	120h
2	0.5	9.76	13.5	16.6	24	34.7	60.3	82.7	109	137	152	161	167
5	0.2	13	17.9	22	31.6	45.5	78.9	108	142	177	197	208	215
10	0.1	15.4	21.3	26.1	37.4	53.7	92.8	127	166	207	229	243	251
20	0.05	18	24.8	30.3	43.4	62.2	107	146	191	238	263	278	287
50	0.02	21.5	29.6	36.2	51.7	74	127	173	225	280	309	326	336
100	0.01	24.4	33.5	40.9	58.3	83.2	143	193	252	312	344	363	374
Rainfall depths (mm) :: RCP8.5 for the period 2031-2050													
ARI	AEP	10m	20m	30m	1h	2h	6h	12h	24h	48h	72h	96h	120h
2	0.5	9.38	13	16	23.1	33.4	58.4	80.4	107	134	149	158	164
5	0.2	12.4	17.2	21.1	30.4	43.8	76.3	105	138	173	192	204	211
10	0.1	14.8	20.4	25	35.9	51.6	89.6	123	162	203	224	238	246
20	0.05	17.2	23.7	29	41.6	59.7	103	141	186	232	257	272	281
50	0.02	20.6	28.4	34.7	49.6	71	122	167	219	273	302	319	330
100	0.01	23.4	32.1	39.2	55.8	79.8	137	187	245	304	336	355	367
Rainfall depths (mm) :: RCP8.5 for the period 2081-2100													
ARI	AEP	10m	20m	30m	1h	2h	6h	12h	24h	48h	72h	96h	120h
2	0.5	11.2	15.5	19.1	27.5	39.5	67.5	91.5	119	147	162	171	177
5	0.2	14.9	20.7	25.3	36.4	52.2	89	120	156	192	212	223	230
10	0.1	17.8	24.6	30.1	43.2	61.8	105	142	183	226	248	261	269
20	0.05	20.8	28.6	35	50.2	71.7	122	163	210	260	285	300	308
50	0.02	25	34.3	42	59.9	85.4	144	193	249	306	335	352	362
100	0.01	28.3	38.9	47.4	67.6	96.1	162	217	279	341	374	393	403

Table 6-4: Extreme rainfall projections for Appleby, from HIRDS v4.

Site name	Appleby												
Site ID	G13211												
Rainfall depths (mm) :: Historical Data													
ARI	AEP	10m	20m	30m	1h	2h	6h	12h	24h	48h	72h	96h	120h
2	0.5	8.57	12.5	15.4	21.6	29.5	45.9	58.7	73.2	89.1	98.7	106	111
5	0.2	11.4	16.5	20.3	28.4	38.7	60	76.6	95.2	115	128	137	143
10	0.1	13.5	19.6	24.1	33.6	45.7	70.6	89.9	112	135	149	159	167
20	0.05	15.7	22.8	28	39	52.9	81.5	104	128	155	171	183	192
50	0.02	18.8	27.3	33.4	46.4	62.9	96.6	123	152	183	201	215	225
100	0.01	21.3	30.8	37.7	52.3	70.8	108	137	169	204	225	239	251
Rainfall depths (mm) :: RCP4.5 for the period 2031-2050													
ARI	AEP	10m	20m	30m	1h	2h	6h	12h	24h	48h	72h	96h	120h
2	0.5	9.34	13.6	16.8	23.5	32	49.2	62.4	77.1	93.1	103	110	115
5	0.2	12.4	18.1	22.3	31.1	42.2	64.7	81.8	101	121	134	142	149
10	0.1	14.8	21.5	26.4	36.8	49.9	76.2	96.2	118	142	156	166	174
20	0.05	17.3	25	30.7	42.8	57.9	88.2	111	136	163	180	191	200
50	0.02	20.7	30	36.8	51.1	69	105	132	161	193	212	225	235
100	0.01	23.5	33.9	41.5	57.6	77.6	118	148	180	215	236	251	262
Rainfall depths (mm) :: RCP4.5 for the period 2081-2100													
ARI	AEP	10m	20m	30m	1h	2h	6h	12h	24h	48h	72h	96h	120h
2	0.5	9.83	14.3	17.7	24.8	33.7	51.3	64.8	79.6	95.6	105	112	117
5	0.2	13.1	19.1	23.5	32.8	44.5	67.6	85.1	104	125	137	146	153
10	0.1	15.6	22.7	27.9	38.9	52.6	79.8	100	123	146	161	171	179
20	0.05	18.2	26.4	32.5	45.2	61.1	92.5	116	141	169	185	197	205
50	0.02	21.9	31.7	38.9	54	72.8	110	137	167	199	218	231	241
100	0.01	24.8	35.9	43.9	61	82	123	154	187	222	243	258	269
Rainfall depths (mm) :: RCP8.5 for the period 2031-2050													
ARI	AEP	10m	20m	30m	1h	2h	6h	12h	24h	48h	72h	96h	120h
2	0.5	9.46	13.8	17	23.8	32.4	49.7	63	77.7	93.7	103	110	115
5	0.2	12.6	18.3	22.5	31.5	42.8	65.4	82.5	102	122	134	143	150
10	0.1	15	21.8	26.8	37.3	50.6	77	97.1	119	143	157	168	175
20	0.05	17.5	25.4	31.1	43.4	58.6	89.2	112	137	165	181	192	201
50	0.02	21	30.4	37.3	51.8	69.9	106	133	162	194	213	226	236
100	0.01	23.8	34.4	42.1	58.4	78.7	119	149	182	217	238	253	264
Rainfall depths (mm) :: RCP8.5 for the period 2081-2100													
ARI	AEP	10m	20m	30m	1h	2h	6h	12h	24h	48h	72h	96h	120h
2	0.5	11.3	16.4	20.3	28.4	38.4	57.5	71.6	86.8	103	113	119	125
5	0.2	15.1	22	27.1	37.8	51	76.3	94.7	114	135	148	157	163
10	0.1	18	26.2	32.2	44.9	60.5	90.2	112	135	159	174	184	192
20	0.05	21.1	30.6	37.6	52.3	70.4	105	130	156	184	200	212	220
50	0.02	25.4	36.8	45.1	62.6	84	125	154	184	218	237	250	260
100	0.01	28.8	41.6	51	70.7	94.7	141	173	207	243	265	279	290

Table 6-5: Extreme rainfall projections for Motupiko, from HIRDS v4.

Site name	Motupiko												
Site ID	G12481												
Rainfall depths (mm) :: Historical Data													
ARI	AEP	10m	20m	30m	1h	2h	6h	12h	24h	48h	72h	96h	120h
2	0.5	6.87	9.86	12.1	16.8	23	36.4	47.3	60.5	75.9	85.8	93.3	99.4
5	0.2	9.3	13.3	16.2	22.4	30.4	47.5	61.5	78	97.2	110	119	126
10	0.1	11.2	15.9	19.4	26.7	36.1	56	72.1	91.1	113	127	137	146
20	0.05	13.3	18.7	22.7	31.2	42	64.7	83	104	129	145	156	166
50	0.02	16.2	22.8	27.6	37.6	50.4	76.9	98.1	123	151	168	182	192
100	0.01	18.6	26.1	31.5	42.8	57	86.5	110	137	167	187	201	212
Rainfall depths (mm) :: RCP4.5 for the period 2031-2050													
ARI	AEP	10m	20m	30m	1h	2h	6h	12h	24h	48h	72h	96h	120h
2	0.5	7.49	10.8	13.2	18.3	25	39	50.3	63.7	79.3	89.3	96.9	103
5	0.2	10.2	14.5	17.7	24.5	33.2	51.2	65.7	82.6	102	115	124	131
10	0.1	12.3	17.5	21.2	29.3	39.4	60.4	77.1	96.5	119	133	144	152
20	0.05	14.6	20.6	25	34.3	46	70.1	89	111	136	152	163	173
50	0.02	17.8	25.1	30.3	41.4	55.2	83.4	105	130	159	177	190	201
100	0.01	20.5	28.7	34.6	47.1	62.5	93.9	118	146	177	196	211	222
Rainfall depths (mm) :: RCP4.5 for the period 2081-2100													
ARI	AEP	10m	20m	30m	1h	2h	6h	12h	24h	48h	72h	96h	120h
2	0.5	7.88	11.3	13.9	19.3	26.3	40.7	52.2	65.8	81.5	91.5	99.1	105
5	0.2	10.7	15.3	18.7	25.9	34.9	53.6	68.3	85.4	105	118	127	135
10	0.1	13	18.4	22.4	30.9	41.6	63.3	80.3	100	122	137	147	156
20	0.05	15.4	21.7	26.4	36.2	48.5	73.4	92.7	115	140	156	168	177
50	0.02	18.9	26.5	32.1	43.8	58.3	87.5	110	135	164	182	196	206
100	0.01	21.7	30.4	36.6	49.8	66	98.6	123	151	183	202	217	228
Rainfall depths (mm) :: RCP8.5 for the period 2031-2050													
ARI	AEP	10m	20m	30m	1h	2h	6h	12h	24h	48h	72h	96h	120h
2	0.5	7.58	10.9	13.3	18.6	25.3	39.4	50.8	64.2	79.8	89.8	97.4	103
5	0.2	10.3	14.7	17.9	24.8	33.6	51.8	66.3	83.2	103	115	125	132
10	0.1	12.5	17.7	21.5	29.6	39.9	61.1	77.9	97.3	120	134	144	153
20	0.05	14.8	20.9	25.3	34.7	46.6	70.8	89.8	112	137	153	164	174
50	0.02	18.1	25.4	30.7	41.9	55.9	84.3	106	132	160	178	192	202
100	0.01	20.8	29.1	35.1	47.7	63.4	95	119	147	178	198	212	223
Rainfall depths (mm) :: RCP8.5 for the period 2081-2100													
ARI	AEP	10m	20m	30m	1h	2h	6h	12h	24h	48h	72h	96h	120h
2	0.5	9.03	13	15.9	22.1	30	45.5	57.7	71.7	87.8	98	106	112
5	0.2	12.4	17.6	21.5	29.8	40.1	60.4	76.1	93.8	114	127	136	144
10	0.1	15	21.3	25.9	35.7	47.8	71.6	89.7	110	133	148	159	167
20	0.05	17.8	25.2	30.5	41.9	55.9	83.3	104	127	153	169	181	190
50	0.02	21.9	30.7	37.2	50.7	67.2	99.4	123	149	180	198	212	222
100	0.01	25.2	35.2	42.5	57.8	76.3	112	139	167	200	220	235	246

Table 6-6: Extreme rainfall projections for Lake Rotoiti, from HIRDS v4.

Site name	Lake Rotoiti												
Site ID	F12882												
Rainfall depths (mm) :: Historical Data													
ARI	AEP	10m	20m	30m	1h	2h	6h	12h	24h	48h	72h	96h	120h
2	0.5	6.22	8.72	10.7	15.1	21.5	36.9	51.2	69.7	92.9	108	120	130
5	0.2	8.5	11.8	14.4	20.3	28.7	48.8	67.1	90.8	120	140	154	166
10	0.1	10.3	14.3	17.4	24.4	34.2	57.7	79.1	107	140	163	180	193
20	0.05	12.2	16.9	20.5	28.6	40	67	91.5	123	161	186	205	220
50	0.02	15	20.6	25	34.7	48.1	80.1	109	145	189	218	240	257
100	0.01	17.3	23.7	28.6	39.5	54.7	90.3	122	162	211	242	266	285
Rainfall depths (mm) :: RCP4.5 for the period 2031-2050													
ARI	AEP	10m	20m	30m	1h	2h	6h	12h	24h	48h	72h	96h	120h
2	0.5	6.78	9.51	11.6	16.5	23.3	39.6	54.4	73.5	97	113	125	134
5	0.2	9.3	13	15.8	22.3	31.3	52.5	71.7	96.1	126	146	161	173
10	0.1	11.3	15.7	19.1	26.7	37.3	62.3	84.7	113	148	170	188	201
20	0.05	13.4	18.6	22.5	31.4	43.7	72.6	98.1	130	169	195	214	230
50	0.02	16.5	22.7	27.5	38.1	52.8	86.8	117	154	199	229	251	268
100	0.01	19.1	26.1	31.5	43.5	60	98	131	172	222	255	279	297
Rainfall depths (mm) :: RCP4.5 for the period 2081-2100													
ARI	AEP	10m	20m	30m	1h	2h	6h	12h	24h	48h	72h	96h	120h
2	0.5	7.13	10	12.3	17.4	24.5	41.3	56.5	75.8	99.7	116	128	137
5	0.2	9.81	13.7	16.7	23.5	32.9	55	74.6	99.4	130	150	165	177
10	0.1	11.9	16.5	20.1	28.2	39.4	65.2	88.2	117	152	175	193	206
20	0.05	14.2	19.6	23.8	33.2	46.2	76	102	135	175	201	220	236
50	0.02	17.5	24	29	40.3	55.7	91	122	160	206	236	258	275
100	0.01	20.2	27.6	33.3	46	63.4	103	137	179	230	262	287	306
Rainfall depths (mm) :: RCP8.5 for the period 2031-2050													
ARI	AEP	10m	20m	30m	1h	2h	6h	12h	24h	48h	72h	96h	120h
2	0.5	6.86	9.63	11.8	16.7	23.6	40	54.9	74	97.7	113	125	135
5	0.2	9.42	13.1	16	22.6	31.7	53.1	72.4	96.8	127	147	162	174
10	0.1	11.4	15.9	19.3	27.1	37.8	63	85.5	114	149	172	189	202
20	0.05	13.6	18.8	22.8	31.9	44.3	73.4	99.1	131	171	197	216	231
50	0.02	16.8	23	27.8	38.7	53.5	87.8	118	155	201	230	253	270
100	0.01	19.3	26.4	31.9	44.1	60.8	99.2	133	174	224	256	280	299
Rainfall depths (mm) :: RCP8.5 for the period 2081-2100													
ARI	AEP	10m	20m	30m	1h	2h	6h	12h	24h	48h	72h	96h	120h
2	0.5	8.17	11.5	14	19.9	28	46.3	62.4	82.7	107	124	136	146
5	0.2	11.3	15.8	19.2	27.1	37.8	62	83.1	109	141	162	177	190
10	0.1	13.8	19.1	23.2	32.6	45.3	73.8	98.5	129	166	190	207	222
20	0.05	16.4	22.7	27.5	38.4	53.2	86.2	114	149	191	218	238	253
50	0.02	20.3	27.8	33.7	46.7	64.3	103	136	176	225	256	279	297
100	0.01	23.4	32	38.6	53.4	73.2	117	154	198	251	285	310	329

7 Potential evapotranspiration deficit projections (meteorological drought)

The measure of meteorological drought¹ used in this section is ‘potential evapotranspiration deficit’ (PED). Evapotranspiration is the process where water held in the soil is gradually released to the atmosphere through a combination of direct evaporation and transpiration from plants. As the growing season advances, the amount of water lost from the soil through evapotranspiration typically exceeds rainfall, giving rise to an increase in soil moisture deficit. As soil moisture decreases, pasture production becomes moisture-constrained and evapotranspiration can no longer meet atmospheric demand.

The difference between this demand (evapotranspiration deficit) and the actual evapotranspiration is defined as the ‘potential evapotranspiration deficit’ (PED). In practice, PED represents the total amount of water required by irrigation, or that needs to be replenished by rainfall, to maintain plant growth at levels unconstrained by water shortage. As such, PED estimates provide a robust measure of drought intensity and duration. Days when water demand is not met, and pasture growth is reduced, are often referred to as days of potential evapotranspiration deficit.

PED is calculated as the difference between potential evapotranspiration (PET) and rainfall, for days of soil moisture under half of available water capacity (AWC), where an AWC of 150mm for silty-loamy soils is consistent with estimates in previous studies (e.g. Mullan et al., 2005). PED, in units of mm, can be thought of as the amount of missing rainfall needed in order to keep pastures growing at optimum levels. Higher PED totals indicate drier soils. An increase in PED of 30 mm or more corresponds to an extra week of reduced grass growth. Accumulations of PED greater than 300 mm indicate very dry conditions.

Historic (average over 1986-2005) and future (average over 2031-2050 and 2081-2100) maps for PED are shown in this section. The historic maps show annual accumulated PED in units of mm and the future projection maps show the change in the annual accumulated PED compared with the historic period, in units of mm. Note that the historic maps are on a different colour scale to the future projection maps.

For the historic period (Figure 7-1), the highest PED accumulation is experienced on the coast at Tasman Bay and further inland in the hill country (around and inland of Upper Moutere) (250-300 mm per year, on average). The eastern half of the region experiences larger accumulations of PED than the western half (i.e. more drought potential).

In the future, the amount of accumulated PED is projected to increase across Tasman, particularly for the hill country inland of Tasman Bay (around Motupiko) (Figure 7-2). By 2040, PED is projected to increase by 100-140 mm per year for that part of the region. By 2090 under RCP4.5 increases of 120-140 mm are projected for this area, and under RCP8.5 increases of 180-200 mm of PED are projected. The eastern half of the region is likely to become substantially more drought prone than it is in the historic period, with average annual totals above 300 mm (indicating very dry conditions becoming more common).

¹ Meteorological drought happens when dry weather patterns dominate an area and resulting rainfall is low. Hydrological drought occurs when low water supply becomes evident, especially in streams, reservoirs, and groundwater levels, usually after an extended period of meteorological drought.

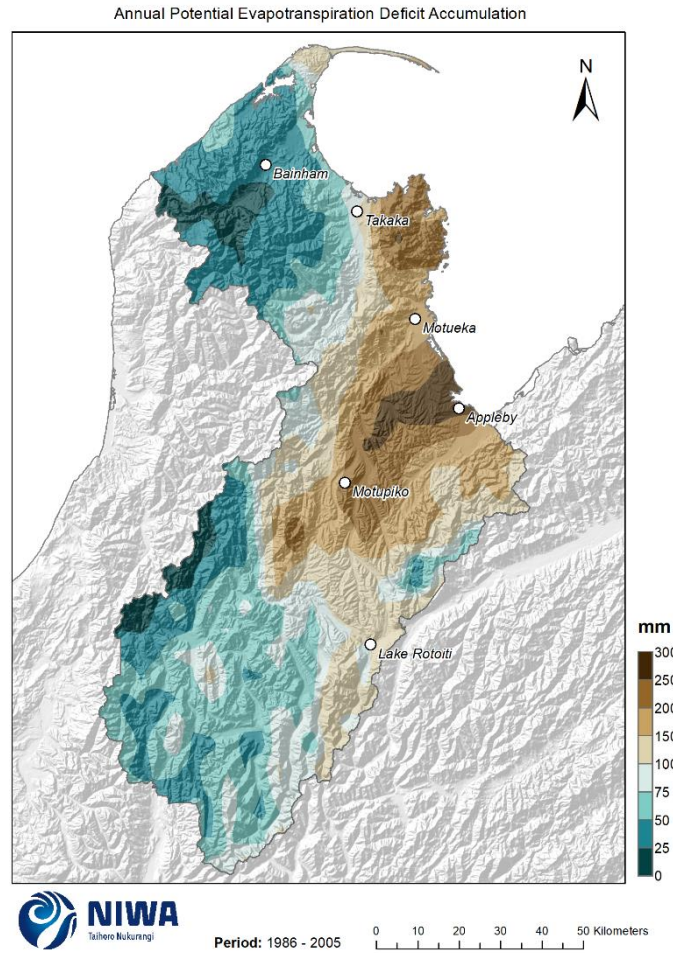


Figure 7-1: Modelled annual accumulated Potential Evapotranspiration Deficit (mm), average over 1986-2005. Results are based on dynamical downscaled projections using NIWA's Regional Climate Model. Resolution of projection is 5km x 5km.

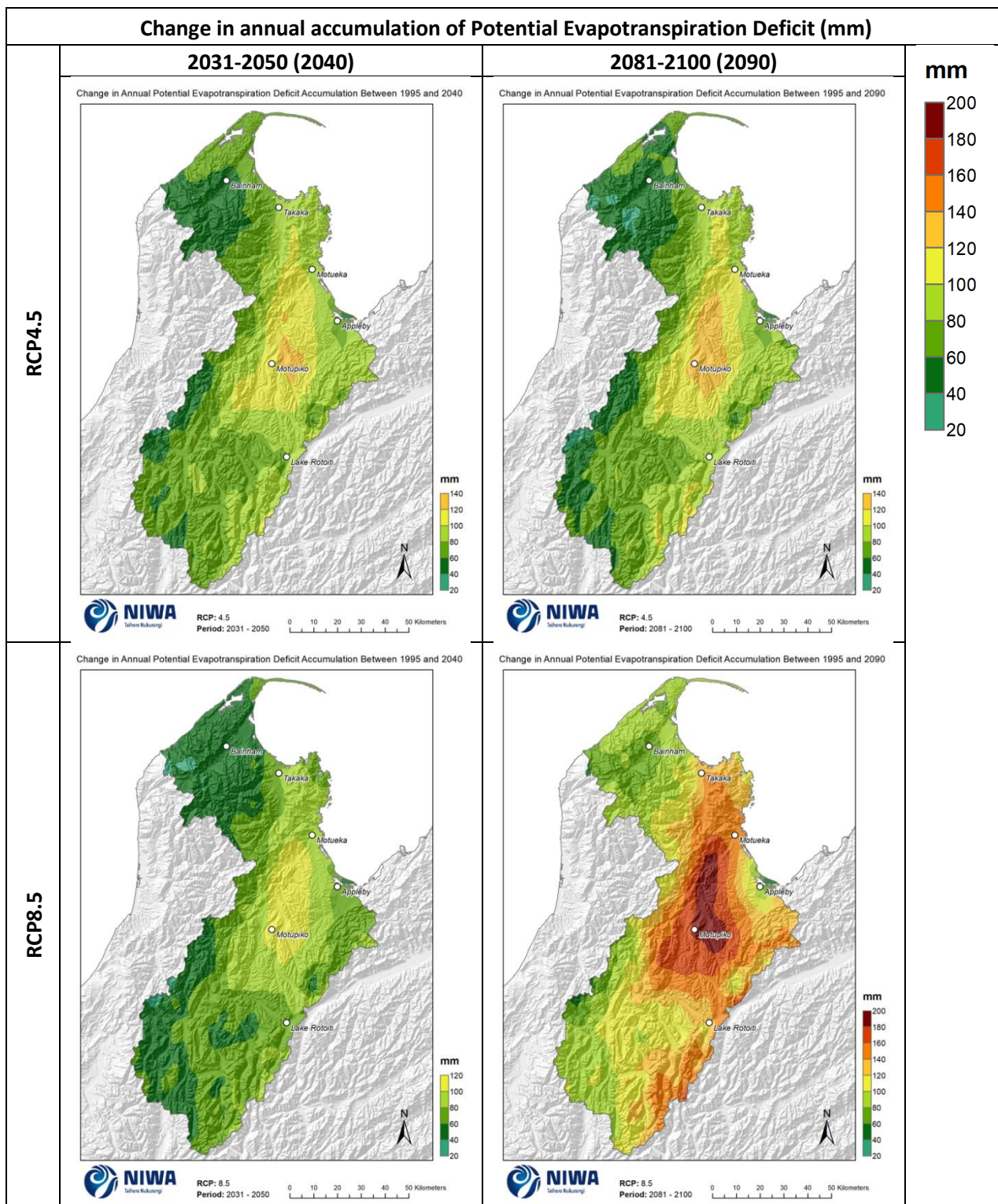


Figure 7-2: Projected annual change in accumulated Potential Evapotranspiration Deficit (mm) at 2040 and 2090. Relative to 1986-2005 average, for RCP4.5 and RCP8.5, based on the average of six global climate models. Results are based on dynamical downscaled projections using NIWA's Regional Climate Model. Resolution of projection is 5km x 5km.

8 Soil moisture deficit day projections

Soil moisture deficit (SMD) is calculated based on incoming daily rainfall (mm), outgoing daily potential evapotranspiration (PET), and a fixed available water capacity of 150 mm (the amount of water in the soil 'reservoir' that plants can use). In the calculation, evapotranspiration continues at its potential rate until about half of the water available to plants is used up (75 mm out of the total 150 mm available). Subsequently, the rate of evapotranspiration decreases, in the absence of rain, as further water extraction takes place. Evapotranspiration is assumed to cease if all the available water is used up (i.e. all 150 mm). A day of SMD is considered in this report to be when soil moisture is below 75 mm of available soil water capacity. The timing of changes in the days of soil moisture deficit projections indicates how droughts may change in timing throughout the year. The PED, that is the cumulative sum of SMD excess over 75 mm threshold, is directly related aridity intensity rather than SMD days measuring duration by counting number of days of exceedence. Thus SMD is measured in days and PED is measured in mm of accumulation, so PED is a more sensitive measure of drought intensity than SMD.

Historic (average over 1986-2005) and future (average over 2031-2050 and 2081-2100) maps for days of SMD are shown in this section. The historic maps show the annual and seasonal number of days of SMD and the future projection maps show the change in the number of days of SMD compared with the historic period. Note that the historic maps are on a different colour scale to the future projection maps.

For the historic period, the highest number of annual SMD days are experienced in the Tasman Bay area and further inland to Motupiko (>200 days per year) (Figure 8-1). The area from Takaka south to Lake Rotoiti experiences 150-200 days of SMD per year. The least number of SMD days is experienced in the Tasman Mountains, with 20-40 days of SMD per year. By season (Figure 8-2), most SMD days are experienced in winter and least in summer.

Future projections of SMD days are presented in Figure 8-3 to Figure 8-10. The number of SMD days is projected to decline for most of the eastern half of the region, particularly in the Waimea Plains. The number of SMD days is projected to increase for the western half of the region. By 2040 under RCP4.5, 15-20 fewer SMD days per year are projected than for the historic period. From Takaka south to Lake Rotoiti, 5-10 fewer SMD days per year are projected than for the historic period. For the western half of the region, 5-10 more SMD days are projected per year. The magnitude of change under RCP8.5 is slightly less than under RCP4.5 by 2040. By 2090 under RCP4.5, most of the region (outside the Waimea Plains) is projected to experience more days of SMD (3-10 more days per year) than for the historic period. The Waimea Plains is projected to experience 5-15 fewer SMD days per year. By 2090 under RCP8.5, those changes are more pronounced with increases of >15 SMD days per year projected for northern, southern and western parts of the region, and >15 fewer SMD days per year projected for the Waimea Plains and surrounding areas.

The overall increases in SMD days in some areas are due to increases predominantly in the summer season and where past values were low. Decreases in the Waimea Plains area are due to decreases in SMD days during winter, autumn and spring. This result, combined with the PED projections, suggests that droughts may become more intense over the summer season in particular, but increasing rainfall at other times of the year may reduce the likelihood of drought occurring then.

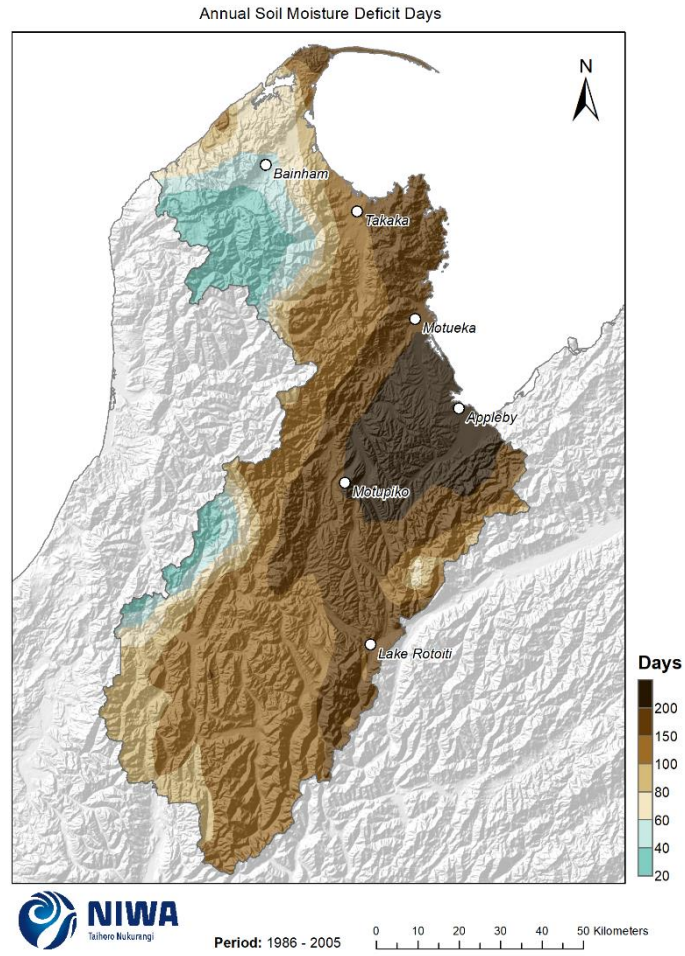


Figure 8-1: Modelled annual number of days of soil moisture deficit (average over the historic period 1986-2005). Based on the average of six global climate models. Results are based on dynamical downscaled projections using NIWA's Regional Climate Model. Resolution of projection is 5km x 5km.

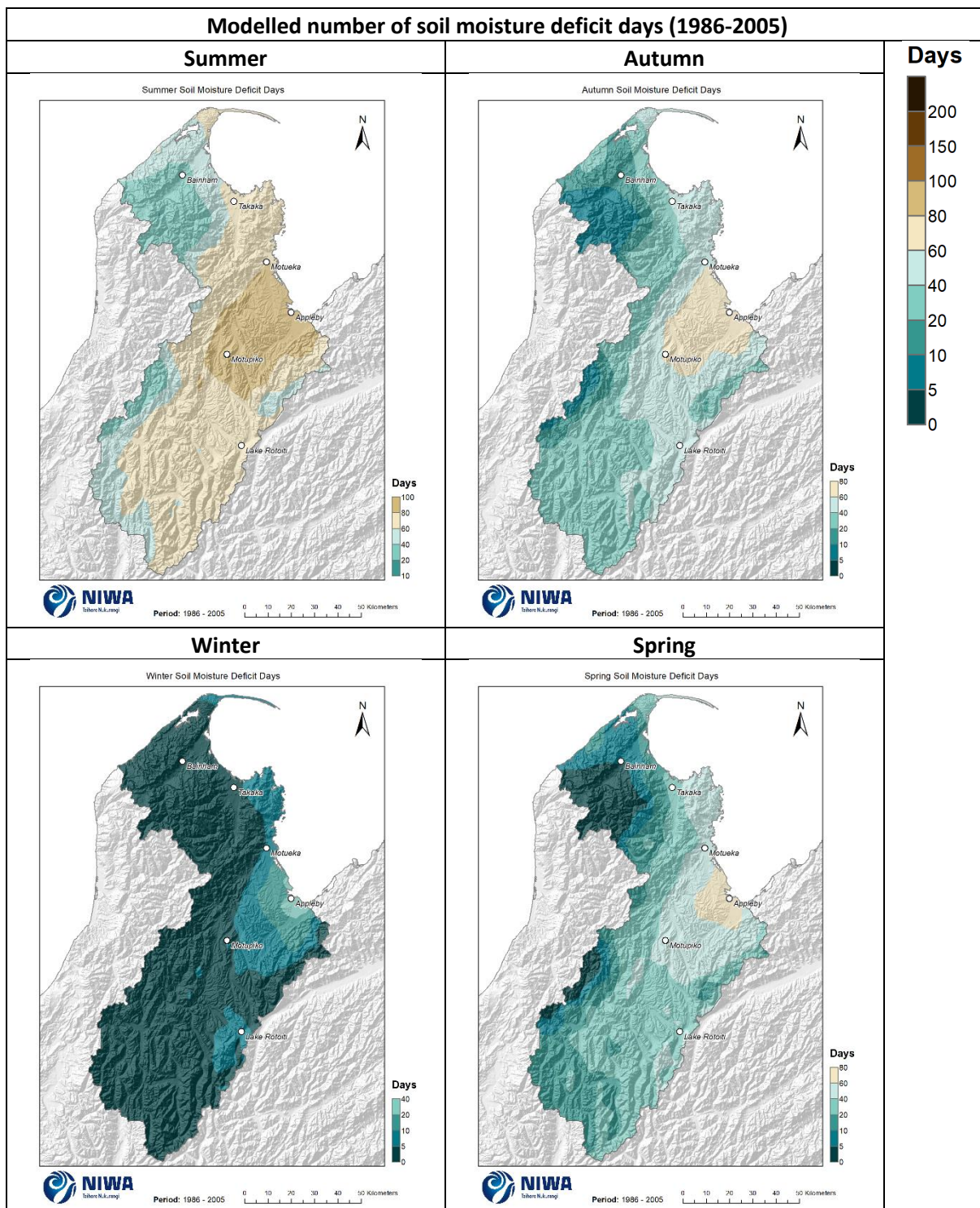


Figure 8-2: Modelled seasonal number of days of soil moisture deficit (average over the historic period 1986-2005). Based on the average of six global climate models. Results are based on dynamical downscaled projections using NIWA's Regional Climate Model. Resolution of projection is 5km x 5km.

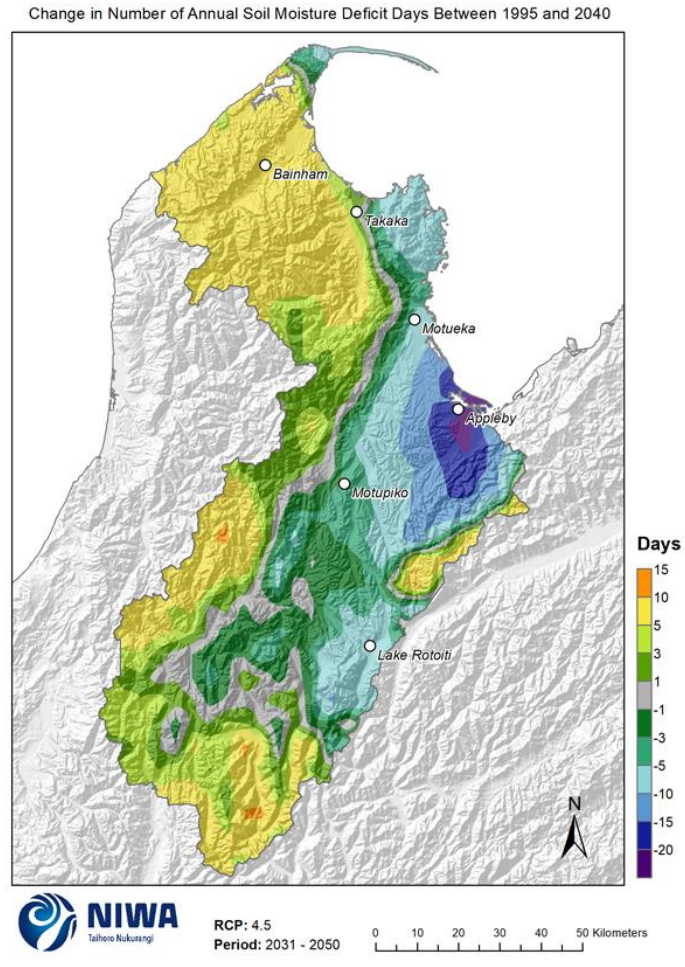


Figure 8-3: Projected change in annual number of days of soil moisture deficit by 2040 for RCP4.5. Relative to 1986-2005 average, based on the average of six global climate models. Results are based on dynamical downscaled projections using NIWA's Regional Climate Model. Resolution of projection is 5km x 5km.

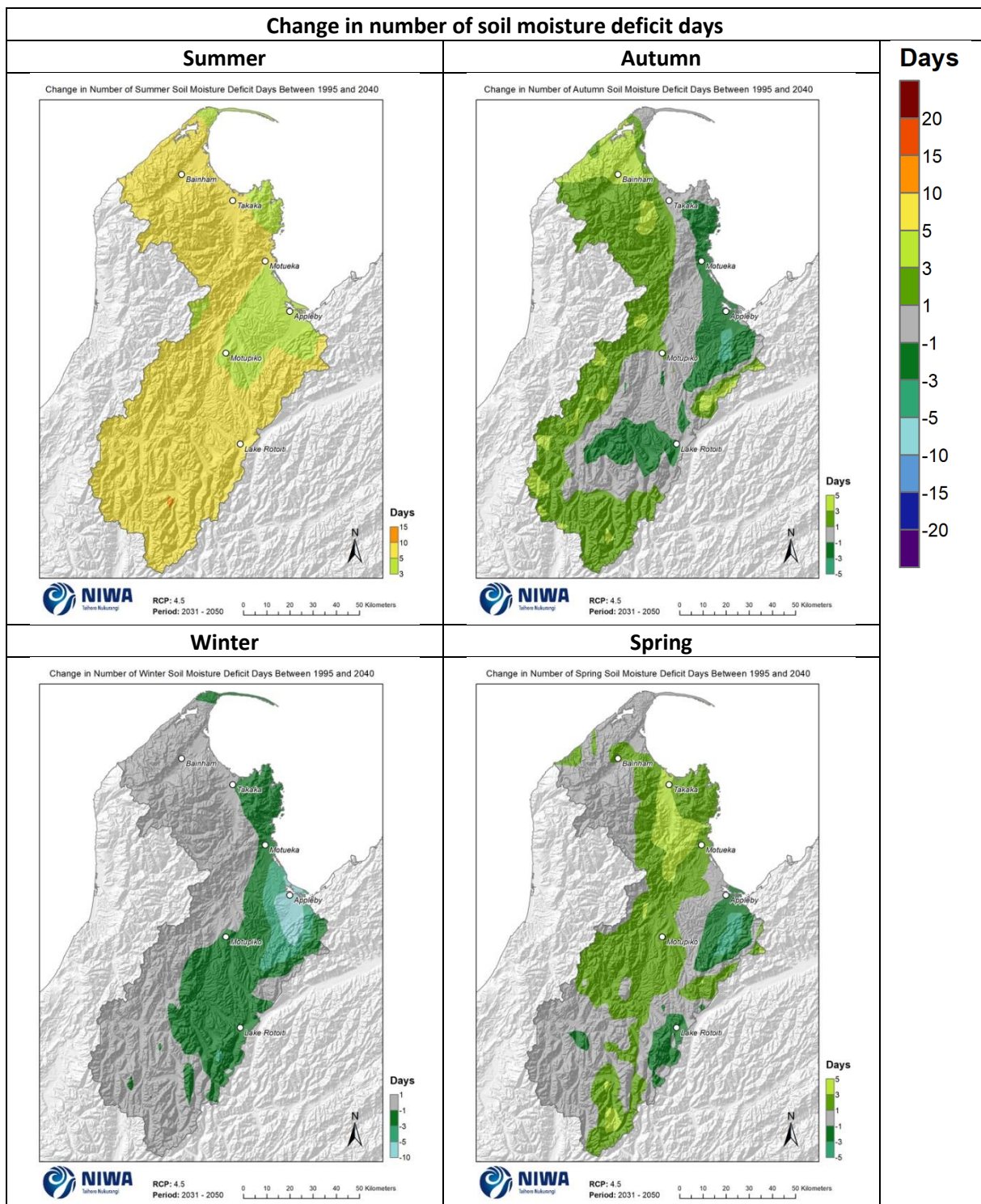


Figure 8-4: Projected change in seasonal number of days of soil moisture deficit by 2040 for RCP4.5. Relative to 1986-2005 average, based on the average of six global climate models. Results are based on dynamical downscaled projections using NIWA's Regional Climate Model. Resolution of projection is 5km x 5km.

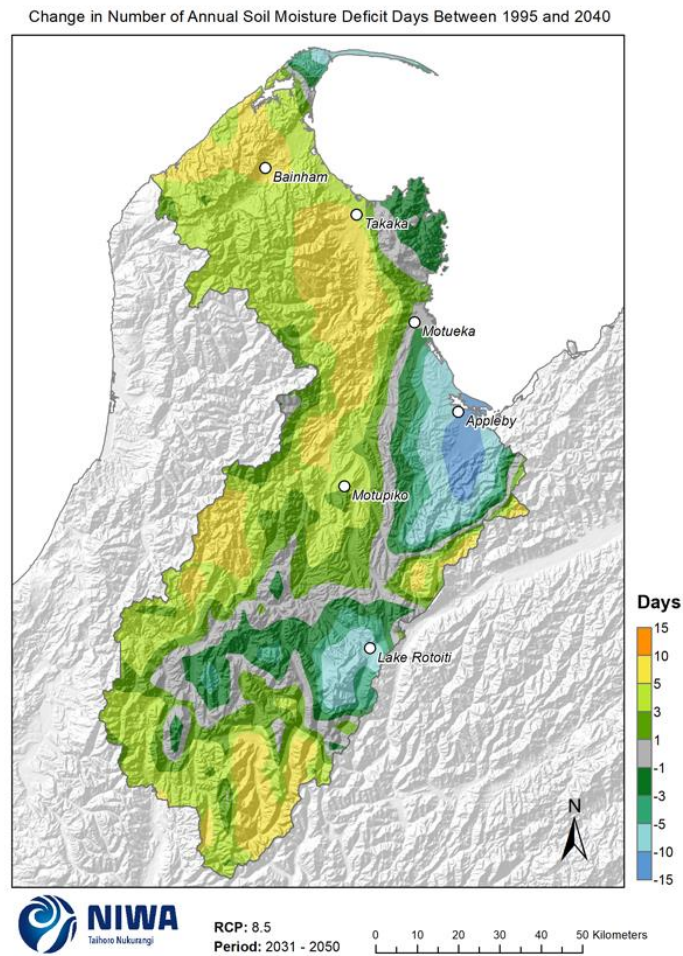


Figure 8-5: Projected change in annual number of days of soil moisture deficit by 2040 for RCP8.5. Relative to 1986-2005 average, based on the average of six global climate models. Results are based on dynamical downscaled projections using NIWA's Regional Climate Model. Resolution of projection is 5km x 5km.

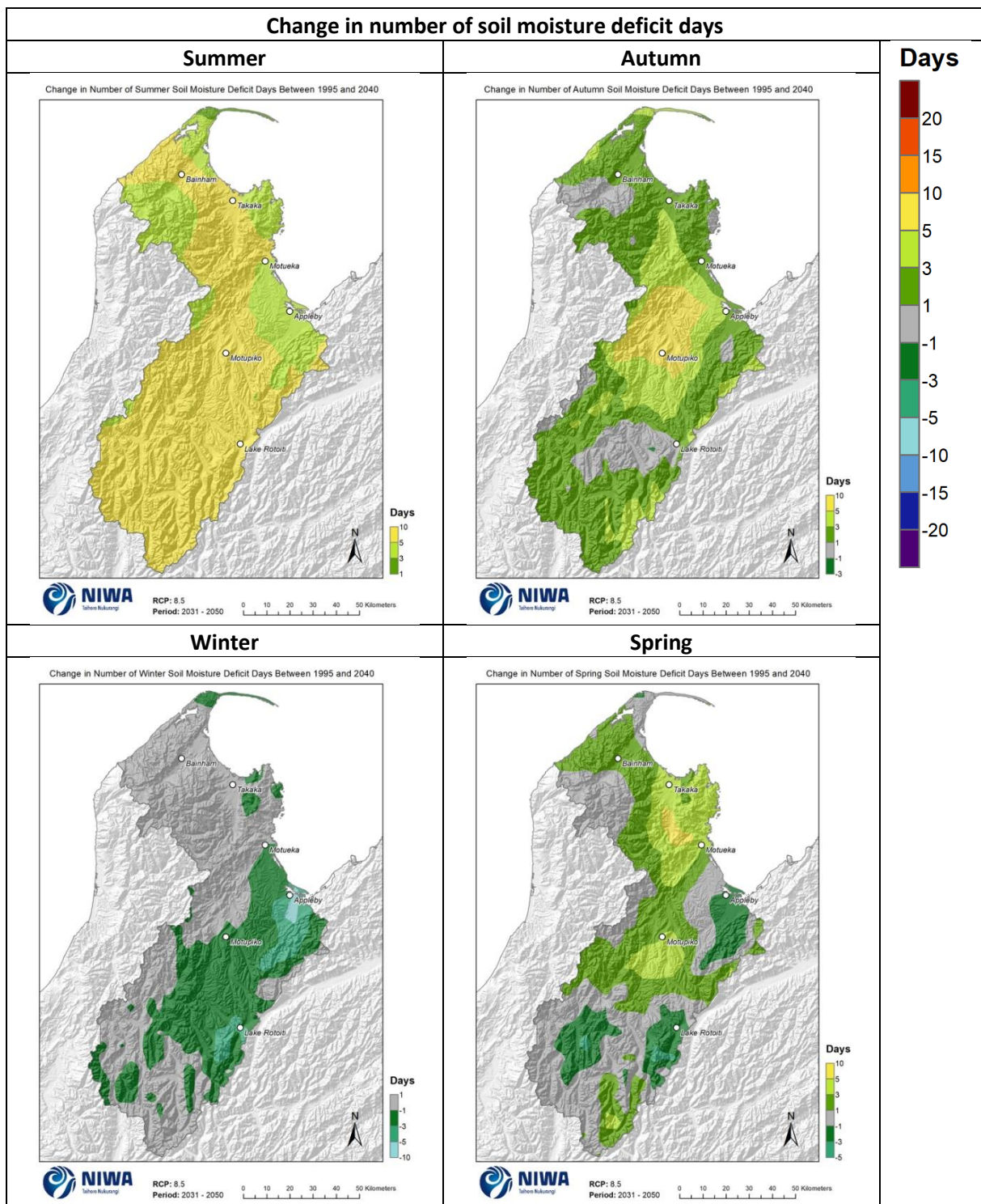


Figure 8-6: Projected change in seasonal number of days of soil moisture deficit by 2040 for RCP8.5. Relative to 1986-2005 average, based on the average of six global climate models. Results are based on dynamical downscaled projections using NIWA's Regional Climate Model. Resolution of projection is 5km x 5km.

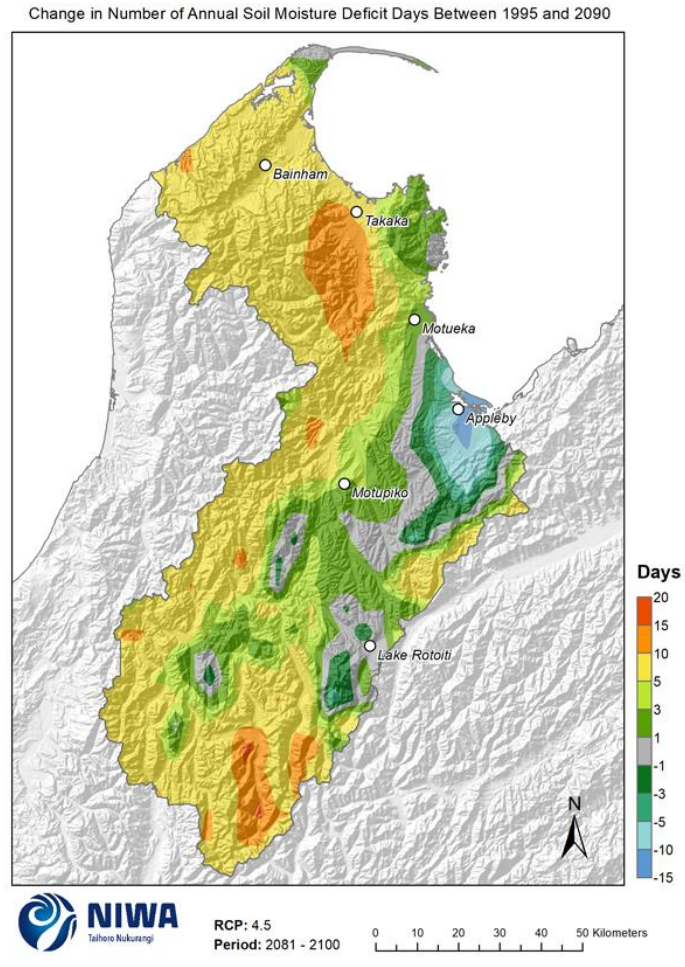


Figure 8-7: Projected change in annual number of days of soil moisture deficit by 2090 for RCP4.5. Relative to 1986-2005 average, based on the average of six global climate models. Results are based on dynamical downscaled projections using NIWA's Regional Climate Model. Resolution of projection is 5km x 5km.

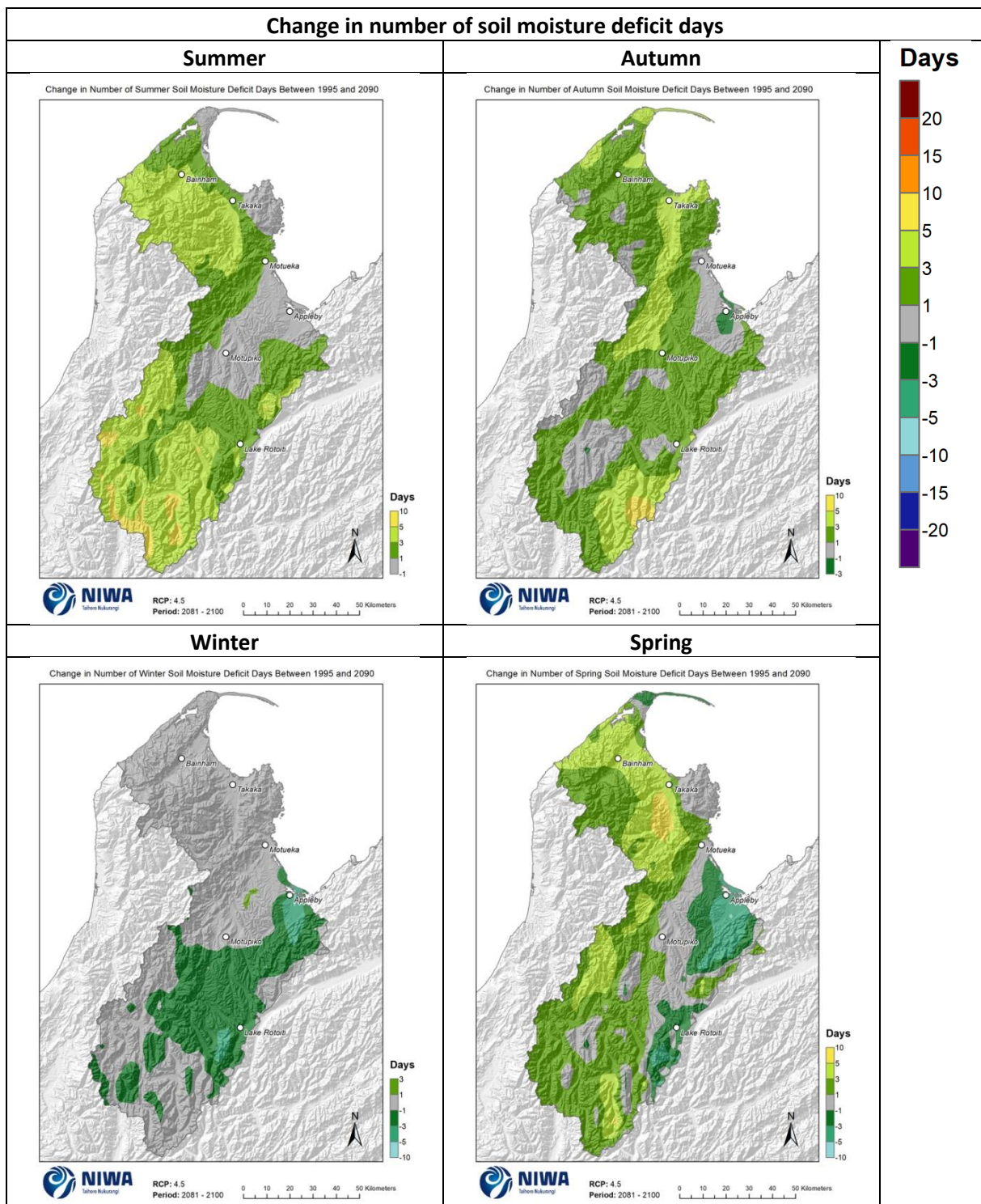


Figure 8-8: Projected change in seasonal number of days of soil moisture deficit by 2090 for RCP4.5. Relative to 1986-2005 average, based on the average of six global climate models. Results are based on dynamical downscaled projections using NIWA's Regional Climate Model. Resolution of projection is 5km x 5km.

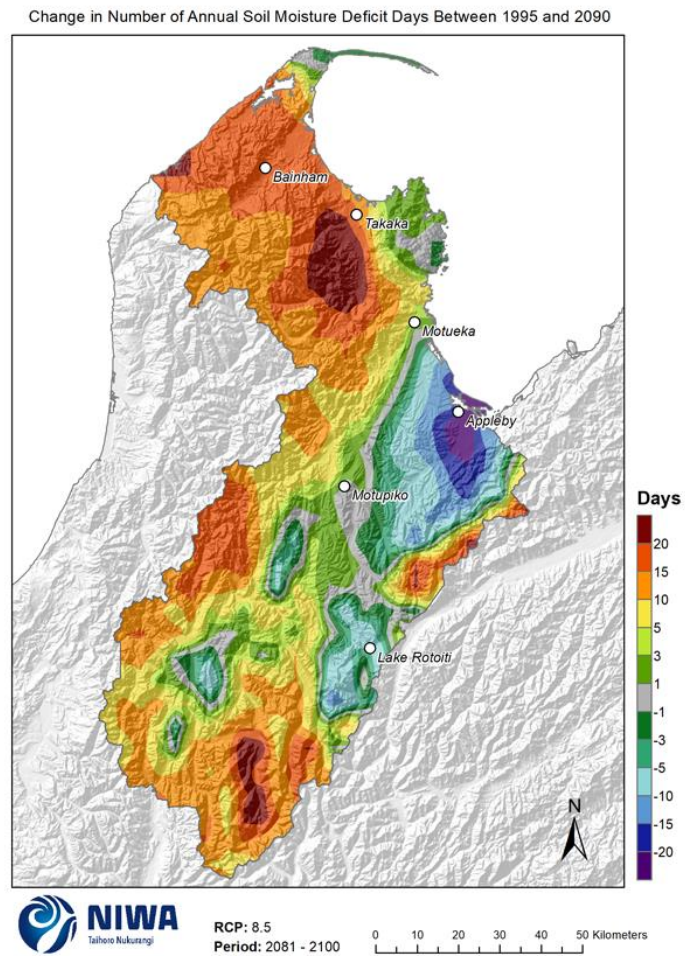


Figure 8-9: Projected change in annual number of days of soil moisture deficit by 2090 for RCP8.5. Relative to 1986-2005 average, based on the average of six global climate models. Results are based on dynamical downscaled projections using NIWA's Regional Climate Model. Resolution of projection is 5km x 5km.

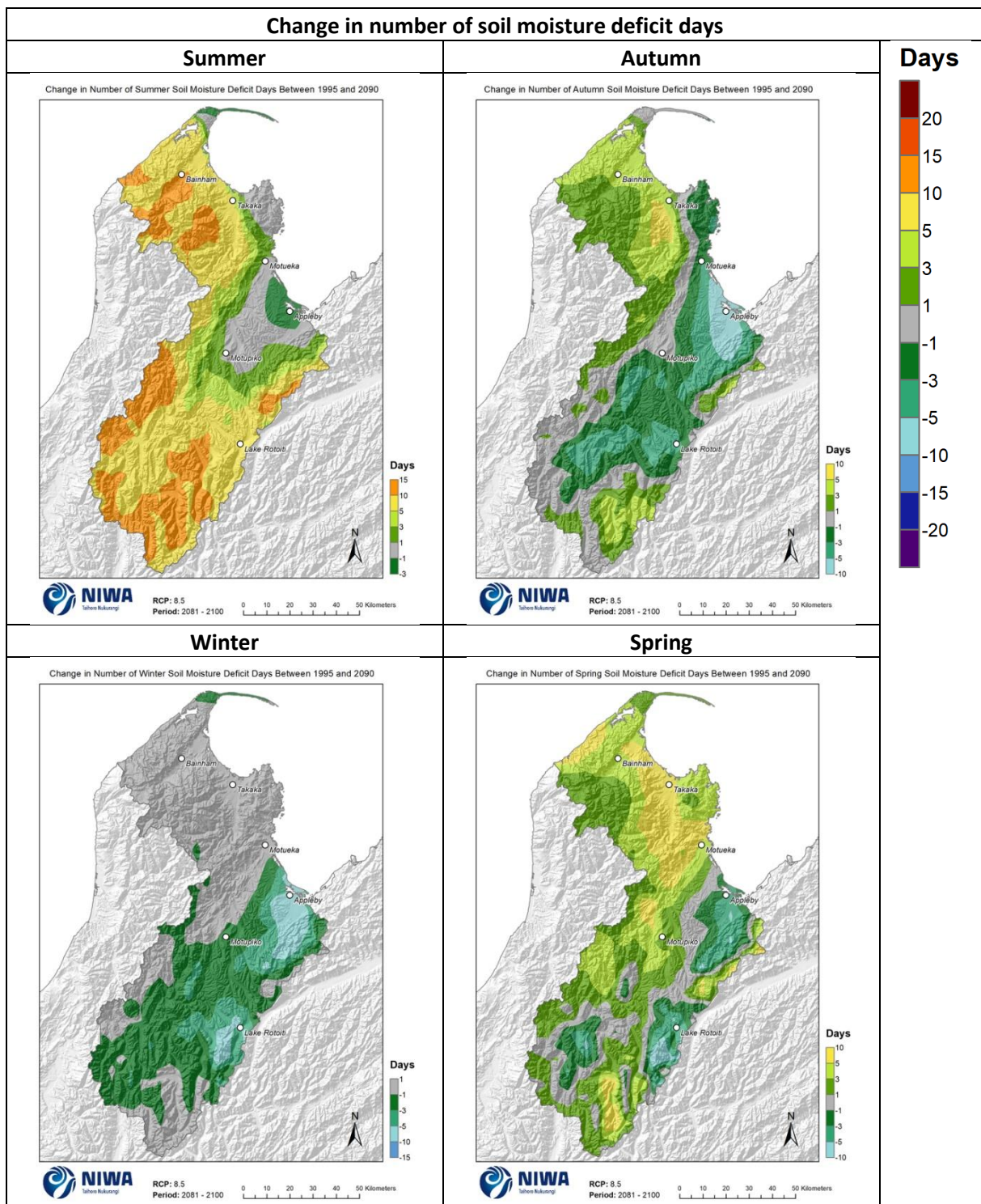


Figure 8-10: Projected change in seasonal number of days of soil moisture deficit by 2090 for RCP8.5. Relative to 1986–2005 average, based on the average of six global climate models. Results are based on dynamical downscaled projections using NIWA's Regional Climate Model. Resolution of projection is 5km x 5km.

9 Climate change impacts on agricultural systems

Tasman District's land classification system is based on climate, topography, soils, and existing/past land use (Agriculture New Zealand, 1994). Eight land classes are defined in Table 9-1, which range from the very flexible land that is suited to many different uses (A), to less flexible land that is only suitable for certain types of land uses or is non-productive (G, H) (more detail provided in Agriculture New Zealand (1994)). Note that a large proportion of the land in Tasman District is excluded from this classification as it is conservation land.

This section provides an overview of potential climate change impacts on agriculture, based on the climate projections presented earlier in this report, the projections of the 2015 NIWA report for TDC, and published literature.

Table 9-1: Tasman District's productive land classes. Refer to Figure 9-1 for map of land classes. After Agriculture New Zealand (1994).

	TDC land class	
Very flexible	A	Very intensive horticulture
	B	Semi-intensive horticulture
	C	Intensive cropping
	D	Cropping
	E	Intensive pastoral
	F	Extensive pastoral
	G	Production forestry
Inflexible	H	Non-productive

Productive Land Classification

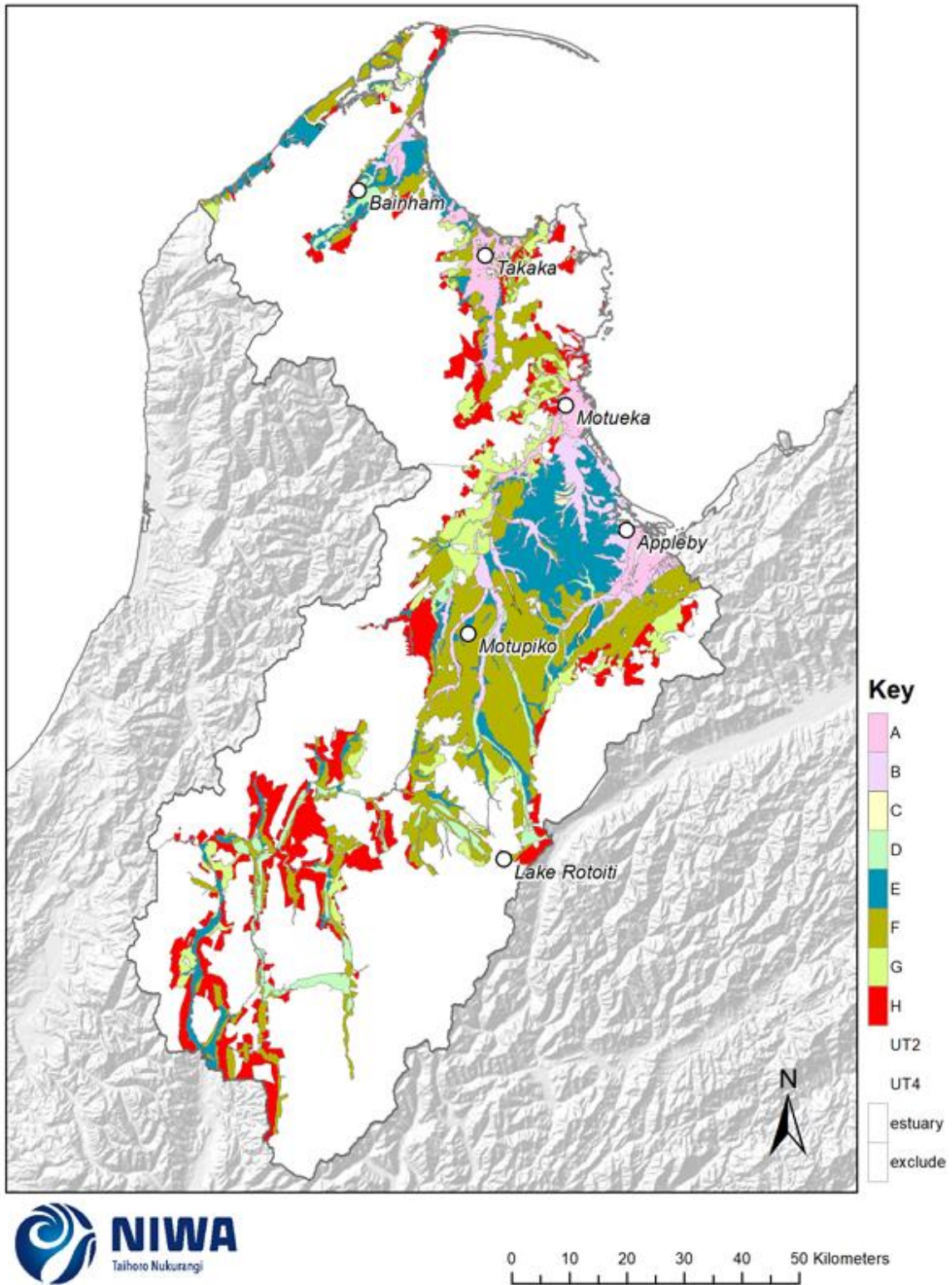


Figure 9-1: Land classes of Tasman District. Refer to Table 9-1 for interpretation of each land class. Note that 'exclude' refers to land that is excluded from this classification system as it is conservation land. After Agriculture New Zealand (1994)

9.1 Heat impacts

New Zealand's maritime climate constrains occurrences of very high temperatures like those observed >40°C in parts of Australia, Europe and the Middle East. However, occurrences of hot days in twenties and thirties are likely to become more frequent in Tasman. This is important because New Zealand's agricultural systems, animals, and plant varieties assume a moderate climate with occasional hot days during summer, and a changing distribution of hot days may impact animal health, plant growth, and the efficiency of those systems.

Animal heat stress may be a future consideration for areas with land suitable for pastoral farming in Tasman. The whole region is projected to experience increased heatwave conditions compared to the historic period, but the southern part of the region is likely to be disproportionately affected (Section 3). Cattle experience heat stress in hot and humid conditions. Generally, the threshold for heat stress for Jersey cows is 25°C. Heat stress results in reduced feed intake, which in turn results in lower milk production (Bryant et al., 2007). Heat can also affect milk composition in terms of proportions of fats and proteins. Farmers may have to consider adaptation strategies like providing more shade, water, and shorter walking distances to milk sheds. As cattle release heat during the night to cool down, increased numbers of warm nights may have a detrimental impact on their ability to do so. However, the risk of heat stress in Tasman is likely to be over a shorter time period during the year than other parts of New Zealand which have a longer warm season (e.g. Northland).

Plant phenological development may occur at a faster rate with increasing extreme heat, which may affect the current agricultural systems in Tasman. Projections of growing degree days (Section 4) show increases across the whole region, but particularly for key areas around Tasman Bay, Takaka, Motupiko and in the far south of the region. Different stages of plant growth (e.g. bud burst, flowering, and fruit development) may happen at different times to present, which may affect the harvested crop. For example, the hottest summer on record for New Zealand in 2017/18 saw wine grapes in multiple New Zealand regions ripen faster than usual (Salinger et al., 2019). In Central Otago, this resulted in the earliest start to harvest of Pinot Noir grapes on record (almost a month earlier than usual). In Wairarapa, the period from flowering to harvest for wine grapes was about 10 days shorter than usual². Some plants require winter chilling for increasing flavour (e.g. carrots) and prompting flowering (e.g. kiwifruit). Reductions in cold temperatures may impact the productivity of these varieties.

However, increasing average temperatures may have positive impacts for forestry as Tasman's climate may become more suitable for *Pinus radiata*, particularly at higher elevations than present (Watt et al., 2018). Reductions in cold conditions and increases in growing degree days may have positive impacts for diversification of new crop or grass varieties that are currently marginal or unviable in Tasman.

Extreme heat affects the rate of evapotranspiration, or the uptake of water by plants. Therefore, increases to extreme heat may affect water availability, as under hot conditions plants use more water than usual. Extreme heat may also result in current varieties of crops and pasture becoming unsustainable if they are not suited to growing in hot conditions.

Increasing risk from pests (plants and animals) and diseases is a concern under a warmer climate. Currently, many pests are limited by cold conditions, so that they cannot survive low winter temperatures, and therefore their spread is limited (Kean et al., 2015). Under a warmer climate,

² <https://michaelcooper.co.nz/2018-regional-vintage-overview-report/>

these pests may not be limited by cold conditions and therefore cause a larger problem for farmers and growers in Tasman.

9.2 Drought impacts

Increased intensity of drought and longer dry spells in parts of Tasman will likely have impacts on water availability for irrigation and other agricultural and horticultural uses.

Low river flows (particularly in summer) are likely to decline in Tasman, with reduced flow reliability (the time period where river water abstraction is unconstrained) (Collins and Zammit, 2016). In addition, potential evapotranspiration deficit (a measure of drought potential) is projected to increase throughout the region (particularly in the central part of Tasman around Motupiko), which may further impact pasture and crop growth and increase the need for irrigation (Section 7). The number of days with soil moisture deficit is projected to decline for the Waimea Plains and eastern parts of the region, but increase in western parts of the region (Section 8). The small decline in soil moisture deficit days for much of the region is due to increasing winter rainfall across the region.

Considering the projections for PED, SMD and rainfall together, droughts in Tasman may become more intense and over a larger region, particularly during the summer months.

Assuming increasing carbon dioxide concentrations in the atmosphere throughout the 21st century, the productivity of forestry (e.g. *Pinus radiata*) and pasture is projected to increase throughout most of New Zealand (Rutledge et al., 2017). However, the increase in productivity may be offset by reduced water availability and increasing summer drought conditions in parts of Tasman. Along with increasing summer drought conditions and potentially more vigorous forest growth, fire risk may increase in the region.

9.3 Heavy rainfall impacts

Increases in extreme rainfall event magnitudes (Section 6) may impact agriculture systems in several different ways. Slips on hill country farmland and deforested areas may become more prevalent during these events, and soil erosion may also be exacerbated by increasing drought conditions (Basher et al., 2012). This has impacts on the quality of soil for agriculture, the area of land available for production, and other impacts such as sedimentation of waterways (which can impact flooding and water quality). Slips may also impact transport infrastructure (e.g. roads, farm tracks) which may in turn affect connectivity of farms and orchards to markets.

High rainfall will impact soil moisture, and saturated soils may be detrimental for different types of agriculture. Pugging by animals occurs when soils are saturated, which compacts soil and damages soil structure, leading to reduced pasture production and increased runoff. Wet soils may cause issues for vegetable growers in particular, as crops may get washed away or the lack of oxygen around the plants may reduce their growth rate. Heavy rain at harvest times for fruit may cause a decline in fruit quality, with skins splitting and increased prevalence of diseases.

Storms with tropical origins (e.g. ex-tropical cyclones) regularly affect Tasman and are associated with high amounts of rainfall (e.g. ex-tropical cyclone Gita in 2017 severely affected the Takaka area). Research suggests that the number of tropical cyclones may slightly decrease in the future, but these storms are likely to produce more extreme rainfall (Patricola and Wehner, 2018). At this stage the number of ex-tropical cyclones that may affect New Zealand in the future is uncertain, but the intensity of these storms is projected to increase consistent with global projections.

10 Summary

Future climate changes depend on the pathway taken by the global community (i.e. through mitigation of greenhouse gas emissions or a 'business as usual' approach). The global climate system will respond differently to future pathways of greenhouse gas concentrations. The representative concentration pathway approach taken here reflects these differences through the consideration of multiple scenarios (i.e. RCP4.5, the mid-range scenario, and RCP8.5, the business-as-usual scenario).

Overall, Tasman will likely experience a warmer, wetter climate with increased seasonal climate extremes. Drought intensity may increase in the summer and heavy rainfall may increase in the winter and spring. Ex-tropical cyclones will continue to affect the region from time to time, and the rainfall intensity from those systems may increase. Frost incidence is likely to fall, and the occurrence of high temperatures and heatwaves will increase.

These changes to Tasman's climate are likely to have impacts on the agricultural systems in the region. The highly flexible land classes in coastal lowland areas such as Waimea Plains, around Motueka and Takaka, and in valleys further inland, are already the warmest parts of the region and will become warmer in the future. This may have impacts on the land uses and crop types that are currently grown in these areas. For less flexible land (e.g. around Motupiko, Lake Rotoiti and Bainham), if these areas are limited by cold conditions rather than other factors such as soil type and topography, future warming presents an opportunity for these areas to become more flexible. Increasing drought intensity across the region, but particularly in central areas, in summer may impact pasture and crop growth and increase the need for irrigation, as well as increasing fire risk in forested areas. Winter rainfall in particular is projected to increase, and extreme rainfall events may increase in intensity, potentially causing more slips on hill country farmland and deforested areas.

11 References

- AGRICULTURE NEW ZEALAND 1994. Classification system for productive land in the Tasman District, Report prepared for Tasman District Council, 88p.
- BASHER, L., ELLIOTT, S., HUGHES, A., TAIT, A., PAGE, M., ROSSER, B., MCIVOR, I., DOUGLAS, G. & JONES, H. 2012. Impacts of climate change on erosion and erosion control methods - A critical review. MPI Technical Paper No: 2012/45, 216pp.
- BRYANT, J. R., LÓPEZ-VILLALOBOS, N., PRYCE, J. E., HOLMES, C. W. & JOHNSON, D. L. 2007. Quantifying the effect of thermal environment on production traits in three breeds of dairy cattle in New Zealand. *New Zealand Journal of Agricultural Research*, 50, 327-338.
- CAREY-SMITH, T., HENDERSON, R. & SINGH, S. 2018. High Intensity Rainfall Design System Version 4, NIWA Client Report 2018022CH.
- COLLINS, D. & ZAMMIT, C. 2016. Climate change impacts on agricultural water resources and flooding. NIWA Client Report for the Ministry of Primary Industries, 2016144CH, 70p.
- FISCHER, E. M. & KNUTTI, R. 2016. Observed heavy precipitation increase confirms theory and early models. *Nature Clim. Change*, 6, 986-911, doi:10.1038/nclimate3110.
- KEAN, J. M., BROCKERHOFF, E. G., FOWLER, S. V., GERARD, P. J., LOGAN, D. P., MULLAN, A. B., SOOD, A., TOMPKINS, D. M. & WARD, D. F. 2015. Effects of climate change on current and potential biosecurity pests and diseases in New Zealand. Prepared for Ministry for Primary Industries, MPI Technical Paper No: 2015/25. 100p.
- MULLAN, A. B., PORTEOUS, A., WRATT, D. & HOLLIS, M. 2005. Changes in drought risk with climate change. NIWA report WLG2005-23 for Ministry for the Environment and Ministry of Agriculture and Fisheries, Wellington.
- PATRICOLA, C. M. & WEHNER, M. F. 2018. Anthropogenic influences on major tropical cyclone events. *Nature*, 563, 339-346.
- RUTLEDGE, D., AUSSEIL, A.-G., BAISDEN, T., BODEKER, G., BOOKER, D. J., CAMERON, M., COLLINS, D., DAIGENAU, A., FERNANDEZ, M., FRAME, B., KELLER, E., KREMSER, S., KIRSCHBAUM, M., LEWIS, J., MULLAN, A. B., REISINGER, A., SOOD, A., STUART, S., TAIT, A., TEIXEIRA, E. I., TIMAR, L. & ZAMMIT, C. 2017. Identifying feedbacks, understanding cumulative impacts and recognising limits: A national integrated assessment. Synthesis Report RA3. Climate Changes, Impacts and Implications for New Zealand to 2100. MBIE contract C01X1225, 84pp.
- SALINGER, M. J., RENWICK, J., BEHRENS, E., MULLAN, A. B., DIAMOND, H. J., SIRGUEY, P., SMITH, R. O., TROUGHT, M. C. T., ALEXANDER, L., CULLEN, N., FITZHARRIS, B. B., HEPBURN, C. D., PARKER, A. K. & SUTTON, P. J. H. 2019. The unprecedented coupled ocean-atmosphere summer heatwave in the New Zealand region 2017/18: drivers, mechanisms and impacts. *Environmental Research Letters*, 14.
- TRENBERTH, K. E. 1999. Conceptual framework for changes of extremes of the hydrological cycle with climate change. *Climatic Change*, 42, 327-339, doi:10.1023/A:1005488920935.
- WATT, M. S., KIRSCHBAUM, M., MOORE, J. R., PEARCE, H. G., BULMAN, L. S., BROCKERHOFF, E. G. & MELIA, N. 2018. Assessment of multiple climate change effects on plantation forests in New Zealand. *Forestry*, 92.

Appendix A Climate modelling methodology

NIWA has used climate model simulation data from the IPCC Fifth Assessment to update climate change scenarios for New Zealand through both regional climate model (dynamical) and statistical downscaling processes. The downscaling processes are described in detail in a climate guidance manual prepared for the Ministry for the Environment (2018a), but a short explanation is provided below. Dynamical downscaling results are presented for all variables in this report.

Global climate models (GCMs) are used to make future climate change projections for each future scenario, and results from these models are available through the Fifth Coupled Model Inter-comparison Project (CMIP5) archive (Taylor et al., 2012). Six GCMs were selected by NIWA for dynamical downscaling, and the sea surface temperatures (SSTs) from these six CMIP5 models used to drive an atmospheric global model, which in turn drives a higher resolution regional climate model (RCM) nested over New Zealand. These CMIP5 models were chosen because they produced the most accurate results when compared to historical climate and circulation patterns in the New Zealand and southwest Pacific region. In addition, they were chosen because they were as varied as possible in the parent global model to span the likely range of model sensitivity. For climate simulations, dynamical downscaling utilises a high-resolution climate model to obtain finer scale detail over a limited area based on a coarser global model simulation.

The six GCMs chosen for dynamical downscaling were BCC-CSM1.1, CESM1-CAM5, GFDL-CM3, GISS-E2-R, HadGEM2-ES and NorESM1-M. The NIWA downscaling (GCM then RCM) produced simulations that contained hourly precipitation results from 1970 through to 2100. The native resolution of the regional climate model is 27 km and there are known biases in the precipitation fields derived from this model. The daily precipitation projections, as well as daily maximum and minimum temperatures, have been bias-corrected so that the temporal distributions from the RCM are consistent with those from the Virtual Climate Station Network (VCSN) when the RCM is driven by the observed sequence of weather patterns across New Zealand (known as 're-analysis' data). When the RCM is driven from the free-running GCM, forced only by CMIP5 SSTs, there can be an additional bias in the distribution of weather patterns affecting New Zealand, and the RCM output data for the historical climate will therefore not match the observed distributions exactly.

The RCM output is then downscaled statistically (by interpolation from the model 27 km grid) to a ~5 km x ~5 km resolution with a daily time-step. The ~5 km grid corresponds to the VCSN grid³. Figure 11-1 shows a schematic for the dynamical downscaling method used in this report.

³ Virtual Climate Station Network, a set of New Zealand climate data based on a 5 km by 5 km grid across the country. Data have been interpolated from 'real' climate station records (TAIT, A., HENDERSON, R., TURNER, R. & ZHENG, X. G. 2006. Thin plate smoothing spline interpolation of daily rainfall for New Zealand using a climatological rainfall surface. *International Journal of Climatology*, 26, 2097-2115.)

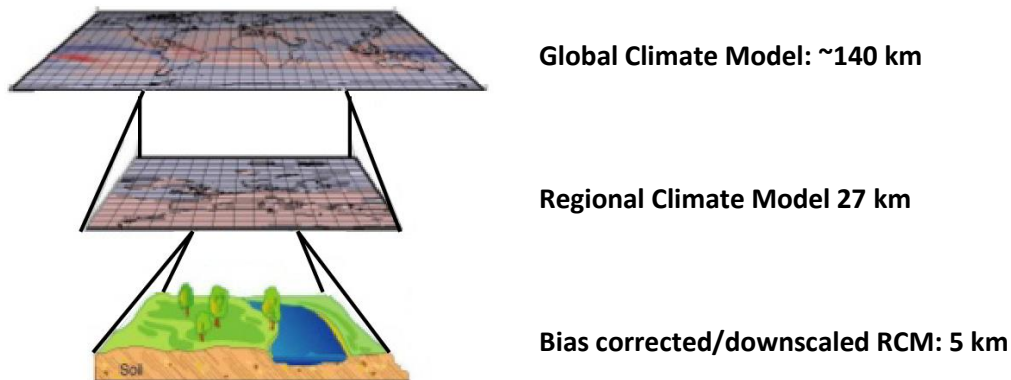


Figure 11-1: Schematic showing dynamical downscaling method used in this report.

The climate change projections from each of the six dynamical models are averaged together, creating what is called an ensemble-average. The ensemble-average is mapped in this report, because the models were chosen to cover a wide range of potential future climate conditions. The ensemble-average was presented as this usually performs better in climate simulations than any individual model (the errors in different models are compensated).

Climate projections are presented as a 20-year average for two future periods: 2031-2050 (termed '2040') and 2081-2100 (termed '2090'). All maps show changes relative to the baseline climate of 1986-2005 (termed '1995'), as used by IPCC. Hence the projected changes by 2040 and 2090 should be thought of as 45-year and 95-year projected trends. Note that the projected changes use 20-year averages, which will not entirely remove effects of natural variability. The baseline maps (1986-2005) show modelled historic climate conditions from the same six models as the future climate change projection maps.

Appendix B Representative Concentration Pathways

Key messages

- Future climate change projections are considered under four emission scenarios, called Representative Concentration Pathways (RCPs) by the IPCC.
- The four RCPs project different climate futures based on future greenhouse gas concentrations, determined by economic, political and social developments during the 21st century.
- RCP2.6 is a mitigation scenario requiring significant reduction in greenhouse gas emissions, RCP4.5 and RCP6.0 are mid-range scenarios where greenhouse gas concentrations stabilise by 2100, and RCP8.5 is a 'business as usual' scenario with greenhouse gas emissions continuing at current rates.
- Projections for the future climate in Tasman District are presented for RCP4.5 and RCP8.5 in this report.

Assessing possible changes for our future climate due to human activity is difficult because climate projections depend strongly on estimates for future greenhouse gas concentrations. Those concentrations depend on global greenhouse gas emissions that are driven by factors such as economic activity, population changes, technological advances and policies for sustainable resource use. In addition, for a specific future trajectory of global greenhouse gas emissions, different climate model simulations produced somewhat different results for future climate change.

This range of uncertainty has been dealt with by the IPCC through consideration of 'scenarios' that describe concentrations of greenhouse gases in the atmosphere. The wide range of scenarios are associated with possible economic, political, and social developments during the 21st century, and via consideration of results from several different climate models for any given scenario. In the 2013 IPCC Fifth Assessment Report, the atmospheric greenhouse gas concentration components of these scenarios are called Representative Concentrations Pathways (RCPs). These are abbreviated as RCP2.6, RCP4.5, RCP6.0, and RCP8.5, in order of increasing radiative forcing by greenhouse gases (i.e. the change in energy in the atmosphere due to greenhouse gas emissions). RCP2.6 leads to low anthropogenic greenhouse gas concentrations (requiring removal of CO₂ from the atmosphere, also called the 'mitigation' scenario), RCP4.5 and RCP6.0 are two 'stabilisation' scenarios (where greenhouse gas emissions and therefore radiative forcing stabilises by 2100) and RCP8.5 has very high greenhouse gas concentrations (the 'business as usual' scenario). Therefore, the RCPs represent a range of 21st century climate policies. Table 11-1 shows the projected global mean surface air temperature for each RCP.

Table 11-1: Projected change in global mean surface air temperature for the mid- and late- 21st century relative to the reference period of 1986-2005 for different RCPs. After IPCC (2013).

Scenario	Alternative name	2046-2065 (mid-century)		2081-2100 (end-century)	
		Mean	Likely range	Mean	Likely range
RCP2.6	Mitigation scenario	1.0	0.4 to 1.6	1.0	0.3 to 1.7
RCP4.5	Stabilisation scenario	1.4	0.9 to 2.0	1.8	1.1 to 2.6
RCP6.0	Stabilisation scenario	1.3	0.8 to 1.8	2.2	1.4 to 3.1
RCP8.5	Business as usual scenario	2.0	1.4 to 2.6	3.7	2.6 to 4.8

The full range of projected globally-averaged temperature increases for all scenarios for 2081-2100 (relative to 1986-2005) is 0.3 to 4.8°C (Figure 11-2). Warming will continue beyond 2100 under all RCP scenarios except RCP2.6. Warming will continue to exhibit inter-annual-to-decadal variability and will not be regionally uniform.

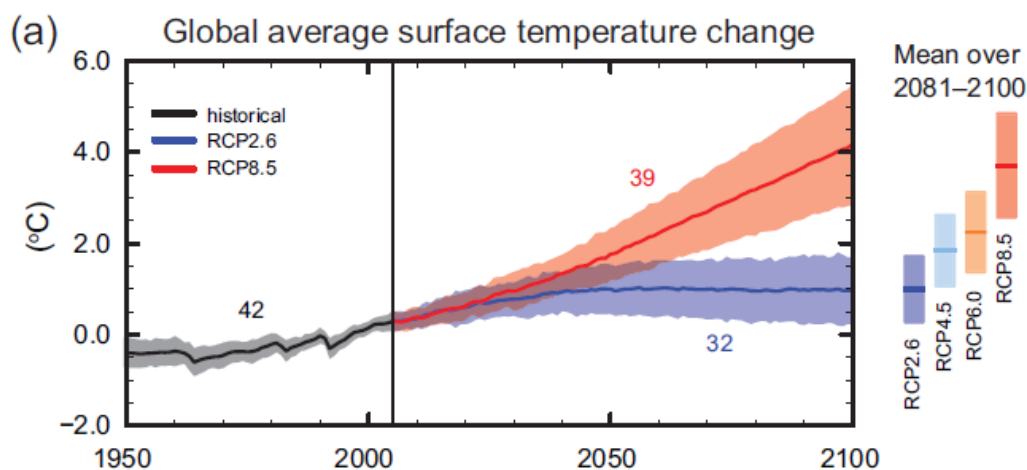


Figure 11-2: CMIP5 multi-model simulated time series from 1950-2100 for change in global annual mean surface temperature relative to 1986-2005. Time series of projections and a measure of uncertainty (shading) are shown for scenarios RCP2.6 (blue) and RCP8.5 (red). Black (grey shading) is the modelled historical evolution using historical reconstructed forcings. The mean and associated uncertainties averaged over 2081-2100 are given for all RCP scenarios as coloured vertical bars to the right of the graph (the mean projection is the solid line in the middle of the bars). The numbers of CMIP5 models used to calculate the multi-model mean is indicated on the graph. From IPCC (2013).

As global temperatures increase, it is virtually certain that there will be more hot and fewer cold temperature extremes over most land areas. It is very likely that heat waves will occur with a higher frequency and duration. Furthermore, the contrast in rainfall between wet and dry regions and wet

and dry seasons will increase. Along with increases in global mean temperature, mid-latitude and wet tropical regions will experience more intense and more frequent extreme rainfall events by the end of the 21st century. The global ocean will continue to warm during the 21st century, influencing ocean circulation and sea ice extent.

Cumulative CO₂ emissions will largely determine global mean surface warming by the late 21st century and beyond. Even if emissions are stopped, the inertia of many global climate changes will continue for many centuries to come. This represents a substantial multi-century climate change commitment created by past, present, and future emissions of CO₂.

In this report, global climate model outputs based on two RCPs (RCP4.5 and RCP8.5) have been downscaled to produce future climate projections for the Tasman District. The rationale for choosing these two scenarios was to present a 'business-as-usual' scenario if greenhouse gas emissions continue at current rates (RCP8.5) and a scenario which could be realistic if global action is taken towards mitigating climate change, for example the Paris climate change agreement (RCP4.5).